

Baffin Island and West Greenland Current Systems in Northern Baffin Bay

Andreas Münchow

College of Earth, Ocean, and Environment, University of Delaware, Newark, DE 19716, U.S.A.

Kelly K. Falkner

National Science Foundation, Arlington, Virginia, U.S.A.

Humfrey Melling

Institute of Ocean Sciences, Sidney, British Columbia, Canada

Abstract

Temperature, salinity, and direct velocity observations from northern Baffin Bay are presented from a summer 2003 survey. The data reveal interactions between fresh and cold Arctic waters advected southward along Baffin Island and salty and warm Atlantic waters advected northward along western Greenland. Geostrophic currents estimated from hydrography are compared to measured ocean currents above 600 m depth. The Baffin Island Current is well constrained by the geostrophic thermal wind relation, but the West Greenland Current is not. Furthermore, both currents are better described as current systems that contain multiple velocity cores and eddies. We describe a surface-intensified Baffin Island Current seaward of the continental slope off Canada and a bottom-intensified West Greenland Current over the continental slope off Greenland. Acoustic Doppler current profiler observations suggest that the West Greenland Current System advected about 3.8 ± 0.27 Sv ($\text{Sv} = 10^6 \text{ m}^3 \text{ s}^{-1}$) towards the north-west at this time. The most prominent features were a surface intensified coastal current advecting 0.5 Sv and a bottom intensified slope current advecting about 2.5 Sv in the same direction. Most of this north-westward circulation turned southward in the Baffin Island Current System. The Baffin Island system was transporting 5.1 ± 0.24 Sv to the south-east at the time that includes additional contributions from Nares Strait to the north (1.0 ± 0.2 Sv) and Lancaster Sound to the east (1.0 ± 0.2 Sv). Net freshwater fluxes were 72 and 187 mSv for the West Greenland and Baffin Island currents, respectively. Empirical uncertainty arises from unknown temporal variations at weekly time scales and perturbations introduced by unresolved eddies. Eddies with 10 km horizontal and 400 m vertical scales were common and recirculated up to 1 Sv. Our 2003 observations represent conditions when the North-Atlantic Oscillation index (NAO) was close to zero. Analysis of historical hydrographic data averaged along isobaths during NAO-positive years reveals a baroclinic circulation in Baffin Bay more intense than 2003 with stronger southward flow of fresher Arctic waters along Baffin Island and stronger northward inflow of saltier Atlantic waters along Greenland. During negative NAO years this cyclonic circulation weakens as evidenced by a 1979 synoptic survey of the hydrography along Baffin Island.

Keywords: Circulation, Arctic, Geostrophy, Baffin Bay, Greenland

1. Introduction

Climate change over the North-Atlantic Ocean causes rising coastal sea level along the US eastern seaboard (Sallenger et al., 2012) and more varied weather (Francis and Vavrus, 2012) which combine to increase the risk of extreme flooding (Lin et al., 2012). Enhanced Arctic freshwater discharge (Serreze et al., 2006), melting of polar ice sheets (Shepherd et al., 2012), and the dramatic decline of Arctic summer sea ice (Kwok and

Rothrock, 2009) all provide evidence of change and positive feedbacks. We here focus on the flux of relative fresh ocean waters from the polar ocean to the south. We use the North-Atlantic Oscillation (NAO) index of Hurrell and Deser (2009) as a metric to place detailed observations from 2003 into a larger climatological context. First, however, we introduce our study area to the west of Greenland via a historical review of available data that relates to circulation.

19 On April 30, 1873 the sealer *Tigress* working off
20 coastal Labrador plucked 12 men, 4 children, and 2
21 women off an ice floe. Fed by two Inuit hunters they
22 had floated on ice for 6 months after the *USS Polaris*
23 abandoned them in Nares Strait to the north of Baffin
24 Bay (Berton, 1988). Inadvertently, they also mapped
25 the surface circulation of western Baffin Bay, travel-
26 ing on ice floes almost 3000 km at an average speed of
27 about 0.2 m/s. Less fortunate were the 1502 passengers
28 who perished aboard the *RMS Titanic* on April 15, 1912
29 when she was sunk by an iceberg off Newfoundland.
30 Most likely, this iceberg originated from Greenland or
31 northern Canada taking a path similar to that of the *Po-*
32 *laris* survivors. The dramatic loss of life in 1912 led
33 to the formation of the International Ice Patrol that was
34 charged with monitoring and predicting the location of
35 ice and icebergs as they enter the busy sea lanes of the
36 North Atlantic Ocean.

37 Starting with the 1928 Marion expedition, LCDR
38 Eward H. "Iceberg" Smith of the US Coast Guard con-
39 ducted pioneering studies of the frigid waters between
40 Canada and Greenland that established the generally
41 southward discharge of ice, icebergs, and buoyant sur-
42 face waters from Baffin Bay via Davis Strait into the
43 North Atlantic. Early hydrographic observations such
44 as those taken during the Marion (Smith, 1931) and
45 Gothaab (Kiilerich, 1939) expeditions in 1928 mapped
46 water temperature and salinity of Baffin Bay, Davis
47 Strait, and the Labrador Sea. Smith (1931) used these
48 data to estimate circulation via geostrophy to predict
49 iceberg motions. Furthermore, Smith (1931) developed
50 a proxy for the North Atlantic Oscillation (NAO) to pre-
51 dict the number of icebergs emanating from Baffin Bay
52 to impact shipping south of Newfoundland via a regres-
53 sion of past observations. He discovered that years of
54 positive NAO correspond to higher iceberg counts off
55 Newfoundland the following year. Dunbar (1951) col-
56 lated early Canadian survey data to map water proper-
57 ties of Baffin and Hudson Bay, Labrador, and western
58 Greenland.

59 Two main circulation features emerge from past hy-
60 drographic, modeling, and mooring studies of Baffin
61 Bay. A cold and buoyant near-surface Baffin Island
62 Current advects Arctic ice, waters, and properties south-
63 ward towards Davis Strait (LeBlond, 1980; Fissel et al.,
64 1982; Tang et al., 2004) and a warm and salty subsurface
65 West Greenland Current advects Atlantic water north-
66 ward towards Cape York in northern Baffin Bay (Bourke
67 et al., 1989; Muench, 1971). A summary and synthesis
68 of mostly Canadian mooring and hydrographic efforts
69 in Baffin Bay from 1978 through 1989 is given by Tang
70 et al. (2004) while Cuny et al. (2005) provides a simi-

lar synthesis for Davis Strait. The net volume flux out of
71 Davis Strait is given as 2.6 ± 1.0 Sv by Cuny et al. (2005)
72 who use current meter mooring records below 150-m
73 and geostrophically estimated velocity shear above this
74 depth. Measurements from a year-long 2004/05 de-
75 ployment resulted in 2.3 ± 0.7 Sv which includes directly
76 measured currents both in the upper 100-m of the water
77 column and on the shelves (Curry et al., 2011). Using
78 only hydrographic observations, Muench (1971) esti-
79 mate the net transport across a section of northern Baf-
80 fin Bay to vary between 1.5-2.7 Sv which agrees with
81 the Davis Strait estimate. Ingram et al. (2002) reviews
82 earlier work in northern Baffin Bay in relation to the
83 North Water polynya (Dumont et al., 2009) and refer-
84 ences Addison (1987) who distinguishes Baffin Island
85 Current volume flux contributions to consist of 0.3 Sv
86 from Nares Strait, 0.3 Sv from Jones Sound, 1.1 Sv
87 from Lancaster Sound, and 0.5 Sv from a recirculating
88 West Greenland Current to give a total southward trans-
89 port of 2.3 Sv. These values represent snapshots based
90 on the generally untested assumptions that the flows at
91 northern passages are both baroclinic and geostrophic.
92 Rudels (2011) fully exploits these assumptions to derive
93 volume and freshwater flux estimates for the entire re-
94 gion to the west of Greenland as well as sensitivities to
95 additional freshwater inputs from Greenland's ice sheet.

96 These earlier measurements provide first descriptions
97 of the larger basin-wide circulation features and ice
98 drift climatology, however, they do not always resolve
99 dynamically relevant vertical and horizontal scales of
100 motions associated with both steeply sloping topogra-
101 phy and baroclinic eddies. Hence it is unclear that
102 geostrophically estimated volume fluxes associated with
103 the cyclonic circulation are adequately resolved at both
104 (small) spatial and (long) temporal scales. For ex-
105 ample, hydrographic observations from which to esti-
106 mate geostrophic shear do not resolve seasonal cycles.
107 These cycles vary substantially across Davis Strait and
108 Baffin Bay in both amplitude and phase (Zweng and
109 Münchow, 2006) on account of different time histo-
110 ries of forcing of the West Greenland and Baffin Island
111 Currents, respectively. Furthermore, the assumption of
112 geostrophic balance is rarely tested and can break down
113 near topography (Rabe et al., 2012).

114 We here discuss and analyze ocean data from the
115 most recent expedition of the US Coast Guard to north-
116 ern Baffin Bay in 2003. We made direct velocity
117 measurements along several sections using a vessel-
118 mounted acoustic Doppler current profiler (ADCP).
119 These data allow evaluation of geostrophically esti-
120 mated currents and, more importantly, they demon-
121 strate mesoscale spatial variability. Enhanced delivery
122

123 of fresher and colder waters from the Arctic along the
124 shelves and slopes of Baffin Island and Labrador con-
125 tributes to vertical stratification as far south as the Gulf
126 of Maine and the Mid-Atlantic Bight where interannual
127 ecosystem variability appears to correlate with upstream
128 conditions (Greene et al., 2008). While our present
129 study cannot address seasonal cycles of the salinity,
130 temperature, and density for lack of sufficient data, we
131 do test the assumption of geostrophy and investigate the
132 spatial scales of velocity, salinity, and density fields in
133 northern Baffin Bay. Our synoptic observations from
134 the 2003 summer surveys reveal that the cyclonic cir-
135 culation exhibits substantial spatial variability in the form
136 of eddies generated via instabilities near sloping topog-
137 raphy.

138 2. Study Area and Data

139 Baffin Bay is a semi-enclosed, seasonally ice-covered
140 basin between northern Canada and Greenland. It is
141 linked to the Atlantic Ocean across a 640 m deep sill
142 in Davis Strait and to the Arctic Ocean via Lancaster
143 Sound, Jones Sound, and Nares Strait with sill depths
144 of about 125, 190, and 220 m, respectively (Melling
145 et al., 2008). Fig. 1 shows locations. These channels
146 and straits vary in minimal width from 320 km (Davis
147 Strait), 65 km (Lancaster Sound), to 25 km (Nares
148 Strait). They thus are generally wider than the local in-
149 ternal deformation radius that is about 10 km (Münchow
150 et al., 2006). Hence even the narrowest channel can
151 accommodate opposing baroclinic flows on each side
152 (LeBlond, 1980). Baffin Bay contains wide and gently
153 sloping shelf areas off Greenland in the east and nar-
154 rower, more steeply sloping shelves off Baffin Island in
155 the west. All shelves are disrupted by deep troughs and
156 canyons that connect the continental slope and basin to
157 the ice caps via fjords in mountainous terrain.

158 We primarily use data from the 2003 expedition of the
159 USCGC Healy to northern Baffin Bay and Nares Strait.
160 This ship contains a 75 kHz phased array ADCP that
161 provides continuous profiles of instantaneous horizontal
162 velocity along the ship track from about 20 m below
163 the sea surface to about 300-600 m depth. For abso-
164 lute positioning we use the ships's military grade p-code
165 differential GPS as well as an AshTech GPS that also
166 provides accurate heading, pitch, and roll information.
167 For details on calibration, performance, and process-
168 ing, we refer to Münchow et al. (2006) and Münchow
169 et al. (2007) where the system, data processing, and
170 results from Nares Strait north of 78N are discussed.
171 We note that data are obtained in 15 m vertical bins
172 every 2 minutes. These data are further averaged in

173 space along the track into roughly 3-km horizontal bins
174 for display as sections. Tidal currents are initially re-
175 moved using predictions from the barotropic model of
176 Padman and Erofeeva (2004) at the location and at the
177 time of our measurements, but prove insufficient off
178 Baffin Island on account of large vertical variations of
179 tidal currents that are not contained in the barotropic
180 model. Instead, we determine tidal ellipse parameters
181 at each vertical bin independently using the method of
182 least squares assuming negligible horizontal variations
183 at sections (Münchow, 2000). Detided currents are ex-
184 trapolated to the surface by fitting detided subsurface
185 velocity profiles to an Ekman layer profile with an eddy
186 viscosity of $0.18 \text{ m}^2/\text{s}$ giving a 50 m thick frictional
187 layer. Münchow et al. (2007) describe, discuss, and
188 evaluate the method and parameter choices. Assuming a
189 random standard error of 1 cm/s for vertically averaged
190 currents due to uncertainties in the reference velocity
191 (from bottom-tracking or GPS), detiding, and surface
192 extrapolation, we find 95% confidence limits for vol-
193 ume transport across sections of about $\pm 0.25 \text{ Sv}$.

All hydrographic data were taken with a SeaBird
911Plus sensor package mounted on a 24 bottle rosette
system with dual temperature and conductivity sensors
that were factory calibrated 3 months prior to their
use in Baffin Bay. An Autosal by Guildline was used
throughout the expedition to compare bottle salinities
with those derived from the SeaBird 911Plus package
to ensure integrity of the CTD data collection. The
2003 data are processed identically to those described in
Münchow et al. (2007) and salinities are accurate within
 ± 0.001 (PSS78).

We collected 30 CTD casts in northern Baffin Bay be-
tween July 26 and August 3 of 2003. Thirteen stations
are on a line emanating southward from Cape York,
Greenland at 76N along longitude 67W to the center
of Baffin Bay. Six stations are distributed across Smith
Sound near 78N latitude. A third section emanating
from northern Baffin Island consists of 11 stations and
connects almost perpendicularly to the Cape York sec-
tion at the center of Baffin Bay near 73N. Our focus
is on properties above 600-m, which roughly coincides
with the sill depth of Davis Strait. All temperatures are
presented as potential temperatures.

In order to place our 2003 data into a larger spatial
and temporal context, we also use temperature, salinity,
and density data collected from 1916 through 2003 in
Baffin Bay as it has been assembled by the U.S. National
Oceanographic Data Center and the Canadian Bedford
Institute of Oceanography (NODC/BIO data). Zweng
and Münchow (2006) describe these data, their distribu-
tion in space and time, and report on a distinct warming

225 trend in central Baffin Bay below Davis Strait sill depths 275
226 and a small, but significant freshening trend of surface 276
227 shelf waters from Nares Strait to Labrador. 277

228 We use the NAO index derived from normalized winter 278
229 sea level pressure differences (December through 279
230 March) between Lisbon, Portugal and Reykjavik, Ice- 280
231 land as a proxy for atmospheric variability over the 281
232 northern hemisphere (Hurrell and Deser, 2009). 282

233 3. The West Greenland Current Regime

234 The data from the zonal Cape York and southern 286
235 Nares Strait sections portray the principal water masses 287
236 with southern and northern signatures, respectively. All 288
237 CTD casts exhibit pronounced subsurface temperature 289
238 maxima at salinities larger than 33.9 psu (Fig. 2) that 290
239 are indicative of waters from the North Atlantic Ocean. 291
240 Following Bacle et al. (2002), we distinguish between 292
241 such water entering our study area from the north via 293
242 Nares Strait, which has subsurface (salinity <33.5 psu) 294
243 temperatures no higher than -0.4°C and water entering 295
244 our study area from the south, wherein the subsurface 296
245 maximum temperature is $+2.0^{\circ}\text{C}$ (Fig. 2). The distinc- 297
246 tion becomes particularly clear for temperatures along 298
247 isopycnals in the $\sigma_t = (27.2, 27.6)\text{ kg m}^{-3}$ range. 299

248 The southern waters with 2.0°C near 34.5 psu are of- 300
249 ten associated with the West Greenland Current. How- 301
250 ever, we find these waters in at least 2 flavors with a 302
251 slightly fresher (and warmer) branch located on the con- 303
252 tinental shelf inshore of the 500 m isobath and a saltier 304
253 (and cooler) branch seaward of this isobath. The ex- 305
254 ception is a single cast of intermediate temperature and 306
255 salinity that represents an anomaly seaward of the 2000 307
256 m isobath. Both the spatial distribution of salinity and 308
257 temperature as well as underway ADCP velocity along 309
258 this section suggest that this is an anti-cyclonic eddy of 310
259 West Greenland shelf waters in deep Baffin Bay. Such 311
260 eddies have not previously been reported in Baffin Bay. 312

261 Fig. 3 shows the density, salinity, and temperature 313
262 along a north-south line that is oriented perpendicular 314
263 to bathymetric contours. The shelf off Cape York slopes 315
264 steeply from 50 m to 400 m within 30 km off the coast, 316
265 flattens for about 40 km to plunge below 2000 m about 317
266 100 km from the coast. The salinity of the surface water 318
267 is lowered by ice melt-water, warmed by insolation, 319
268 and well-mixed to 20 m. Underlying waters are cooler 320
269 than -1.5°C or within about 0.3°C of the freezing point. 321
270 Bourke et al. (1989) refer to this water as the Baffin 322
271 Bay Arctic Water consisting of a mixture of waters im- 323
272 pacted by the annual summer melting and winter freez- 324
273 ing cycle, as well as local runoff from Greenland. Be-
274 low this layer which extends to about 200 m depth, we

find water of about 1.2°C at salinities of about 34.4 psu. Bourke et al. (1989) called this Atlantic Intermediate Water. Within these waters, however, we find two distinct cores with temperatures exceeding 2°C and 1.6°C shoreward and seaward of the 600 m isobath, respectively. Between these cores we find cooler and fresher waters with properties between those seaward and landward of the 600 m isobath (see Fig. 2). Velocity observations discussed below will reveal this to be an anti-cyclonic eddy. Note that the isopycnals are largely flat near the 350 m depth where this feature is most pronounced, i.e., the large lateral temperature and salinity gradients compensate such that the lateral density gradient is small.

If lateral density gradients are small in a geostrophic flow, then we expect vertical gradients of horizontal velocity to be small also. Figs. 4 and 5 display snapshots of the West Greenland Current system, derived via ship-based ADCP survey, both as a section and a vertical average. This current system consists of 1) a surface intensified westward coastal current, 2) a sluggish flow on the shelf, 3) an intense, narrow westward jet over the continental slope that spills onto the shelf near the shelf break, 4) an anti-cyclonic eddy, and 5) a sluggish circulation over the deep Baffin Bay (details to follow). The net transport of this current system above 600 m depth combines to about $3.8 \pm 0.27\text{ Sv}$ with more than 2 Sv carried by a less than 40 km wide slope current that we will refer to as the West Greenland Slope Current.

3.1. Coastal Current

Although our survey of northern Baffin Bay was not designed to resolve baroclinic flows within 10 km of the coast, both the along-shore velocity (Fig. 4) and three casts within 25 km off Cape York, Greenland (Fig. 3) reveal a wedge of warm, buoyant surface waters with salinities less than 33.4 psu and density anomalies less than 27.0 kg m^{-3} . Adjacent to the coast, this buoyant wedge extends to 100 m depth but shoals within 30 km to less than 20 m depth. Relatively large westward flows (reaching 0.2 m s^{-1}) are estimated by extrapolating measured flows below 25 m depth with an Ekman layer profile (Münchow et al., 2007). Similarly large flows (0.17 m s^{-1}) are estimated from Margule's equation that assume geostrophic flow relative to negligible flow below a sloping frontal boundary, e.g., $v = i \times g/f \times \Delta\rho/\rho$ where f is the local Coriolis parameter ($1.41 \times 10^{-4}\text{ s}^{-1}$), g is the constant of gravity (9.81 m s^{-2}), ρ is the density of the dynamically active upper layer (1026 kg m^{-3}), $\Delta\rho$ is the density difference across the density interface (1 kg m^{-3}) which has a slope of i (80 m

325 over 30 km). Geostrophic coastal currents driven by local
 326 buoyancy fluxes are common at both mid-latitudes
 327 (Münchow and Garvine, 1993; Pimenta et al., 2008)
 328 and off Greenland (Bacon et al., 2002; Sutherland and
 329 Pickart, 2008). While the impact of such coastal cur-
 330 rents on basin scale volume flux may be small, about 0.5
 331 Sv here, their potential contribution to freshwater flux
 332 is larger as the swift surface flow carries low salinity
 333 waters far from their origins as coastally trapped flows
 334 (Sutherland et al., 2009).

335 3.2. Shelf Flow

336 The flow seaward of the coastal current varies lit-
 337 tle with depth and is always less than 0.1 m s^{-1} . The
 338 depth-averaged flow is always westward and reaches a
 339 local minimum about midway across the shelf at km-
 340 275 (Fig. 5). The integrated volume flux from the shelf
 341 to this location carries about 0.5 Sv. The waters are
 342 somewhat warmer than waters on the same isopycnal
 343 over the deep basin offshore. The shelf break jet that
 344 we discuss next, spills onto the shelf near the bottom.
 345 Largest subtidal velocities exceeding 0.1 m s^{-1} occur
 346 near the 400 m deep bottom close to the shelf break.

347 3.3. West Greenland Slope Current

348 We find a pronounced westward flow over the conti-
 349 nental slope where the water depth plunges from 600 m
 350 at the shelf break to 2000 m within 30 km. The largest
 351 vertically-averaged velocity occurs at the 600 m isobath
 352 reaching 0.2 m s^{-1} (Fig. 5). This flow is about 40 km
 353 wide at the surface, but it becomes more intense below
 354 200 m depth where it exceeds 0.2 m s^{-1} (Fig. 4). The
 355 shoreward edge of this velocity core coincides with the
 356 subsurface temperature maximum at 350 m depth near
 357 the 500 m isobath (Fig. 3). In the seaward direction the
 358 current extends to the 1500 m isobath. The current is
 359 thus contained entirely over the slope and does not ex-
 360 tend to the foot of the continental slope where the bot-
 361 tom changes its slope from 0.05 to 0.002. We will refer
 362 to this current as the West Greenland Slope Current to
 363 distinguish it from the weaker westward flows on the
 364 shelf. The slope current carries a volume of about 2.0
 365 Sv westward over the top 600 m (Fig. 5).

366 Horizontal density gradients associated with the West
 367 Greenland Slope Current are small, because higher tem-
 368 perature and higher salinity relative to ambient wa-
 369 ters compensate each other with regard to density.
 370 Thus while conventional hydrographic measurements
 371 may trace the origin of waters off western Greenland,
 372 they cannot reveal the geostrophic circulation, because
 373 the West Greenland Slope Current contains a large
 374 barotropic component.

375 The relative vorticity ξ of a geostrophic flow is much
 376 smaller than the planetary vorticity f (Gill, 1982). We
 377 estimate ξ for the vertically averaged flow (Fig. 5) as
 378 $\xi \approx \Delta u / \Delta y \approx 0.1f$ where $f = 1.4 \times 10^{-4} \text{ s}^{-1}$ and
 379 $\Delta u = 0.15 \text{ m s}^{-1}$ is the along-slope velocity difference
 380 over an across-slope distance $\Delta y = 12 \text{ km}$. Since nonlin-
 381 ear inertial effects are scaled by $\xi/f \approx 0.1$, we discern
 382 that they are small relative to Coriolis effects and that
 383 the barotropic flow is in geostrophic balance to first or-
 384 der during our expedition.

385 3.4. Anti-Cyclonic Eddy

386 Seaward of the West Greenland Slope Current near
 387 km-170 both a single CTD cast and the velocity mea-
 388 surements approaching and leaving this location from
 389 south to north reveal anomalous water properties and
 390 ocean currents. Ocean currents change from 0.15 m s^{-1}
 391 westward to 0.15 m s^{-1} eastward over a distance of less
 392 than 20 km just seaward of the continental slope (Figs.
 393 3, 4, and 5). Water between 200 m and 500 m within this
 394 feature is cooler and fresher than adjacent waters. This
 395 signature extends to about 800 m depth (not shown).
 396 The locally depressed isopycnals suggest a clock-wise
 397 geostrophic circulation relative to no flow at greater
 398 depths which is consistent with the observed flow shown
 399 in Fig. 4. We thus interpret our observations to repre-
 400 sent an anti-cyclonic eddy.

401 The almost axisymmetric velocity distribution with a
 402 linear shear of 0.3 m s^{-1} over 10 km suggests an eddy
 403 core with radius $r_m \approx 5 \text{ km}$ in solid-body rotation that
 404 can be modeled as a Rankine vortex (Timmermans et al.,
 405 2008). The Rankine vortex emerges as a particular sim-
 406 ple solution in steady fluids where nonlinear advective
 407 and pressure gradient forces contribute to the dynamics.
 408 For a Rankine vortex the azimuthal velocity increases
 409 from zero at the center of the vortex to a maximum
 410 V_g at r_m (0.15 m s^{-1}) and then decreases with the in-
 411 verse distance from the eddy center, e.g., $v(r) = V_g r / r_m$
 412 for $r \leq r_m$ and $v(r) = V_g r_m / r$ for $r > r_m$. Fig. 5
 413 shows the analytical solution demonstrating that it fits
 414 the observed velocity distribution well both for the 10-
 415 km wide eddy core and at least another 10 km to either
 416 side. The Rankine vortex has a uniform potential vortic-
 417 ity distribution $\Pi = 2V_g / r_m$ for $r \leq r_m$ and zero potential
 418 vorticity for $r > r_m$. An estimate of the Rossby number
 419 $Ro = \Pi / f \approx 0.4$ indicates a nonlinear flow. It recircu-
 420 lates a volume flux of at least 0.5 Sv within its core of
 421 uniform potential vorticity.

4. The Baffin Island Current Regime

4.1. Water Masses

Fig. 6 shows potential temperature salinity relationships above 600 m as well as the measurement locations over bottom topography. Off Baffin Island, the temperature of water between the surface mixed layer and the 33.7 isohaline is almost constant at -1.6°C . The low temperature of this part of the halocline reflects the impact of wintertime freezing within the polynyas of northern Baffin Bay - in Smith, Jones and Lancaster Sounds. As salinities increase towards 34.5 psu, temperature increases towards a maximum of $+1.0^{\circ}\text{C}$ near the $27.6 \sigma_{\theta}$ density surface. Again, these waters are distinct from Nares Strait waters which are almost 2°C cooler. Nevertheless, the warm subsurface waters off Baffin Island are always cooler than those found off western Greenland at similar salinities. We thus identify the West Greenland Current System as the main source of the subsurface waters off Baffin Island which is consistent with the cyclonic circulation in northern Baffin Bay. Waters from Nares Strait are a minor source that modify fresher waters near the surface towards warmer temperatures while saltier waters at depth are modified towards cooler temperatures on density surfaces.

Fig. 7 presents the same data along a section that extends from the coast of Baffin Island near 72°N latitude towards the center of Baffin Bay (Fig. 1). A cold and relatively fresh layer above 300 m depth separates a seasonally warmed 20 m thin surface mixed layer from the warm and salty West Greenland Current waters. At salinities below 33.8 psu, the coldest waters of -1.6°C are remnants of winter waters. Comparing the properties of these waters along isopycnals of Figs. 2 and 6, we find the northern waters along isopycnal surfaces such as the $27.0 \sigma_{\theta}$ warmer (and thus saltier) by almost 0.5°C at a salinity near 33.6. The waters at these salinities in Smith Sound likely contain a larger fraction of Pacific waters that enter the Arctic Ocean via Bering Strait (Woodgate and Aagaard, 2005; Münchow et al., 2007).

4.2. Velocity

The most dramatic feature in Fig. 7, however, are undulating isopycnal excursions that exceed 50 m over 40 km. If the associated baroclinic pressure gradients are balanced by the Coriolis force, then we can estimate the geostrophic velocity field that these isopycnals imply. In Fig. 8 we show these geostrophic (thermal wind) velocities that we reference at 600 m depth to observed ADCP velocities. The reference velocities are always

smaller than 0.1ms^{-1} while the geostrophic surface velocities exceed 0.3ms^{-1} in both northward and southward directions as isopycnals slope upward and downwards towards the east, respectively. Opposing flows are particularly strong about 220 km from the coast where a southward jet exceeds 0.4ms^{-1} adjacent to a northward flow of about 0.2ms^{-1} . We find weak geostrophic flows over both the narrow shelf and steeply sloping continental shelfbreak within 50 km off Baffin Island.

The flow calculated via geostrophy compares favorably to concurrent direct observations of velocity derived via ADCP, shown in Figs. 9 and 10. These direct observations consist of both geostrophic and ageostrophic velocity components. The directly observed flow clearly reveals the strong vertical component of shear above 300 m depth. The largest lateral velocity gradient occurs near the surface between 200 km and 220 km from the coast, where the value changes from about -45 cm/s to $+25 \text{ cm/s}$ in both realizations. Clearly the lateral shear is closely linked to the undulations of density surfaces at this location (Fig. 7). Scaling this velocity difference of $\delta U \approx 0.7 \text{ms}^{-1}$ over $L=20 \text{ km}$ by the Coriolis parameter $f=1.38 \text{ s}^{-1}$, we find a first rough estimate of the Rossby number $R = \delta U / (fL) \approx 0.25$ which indicates that nonlinear inertial effects may contribute to the dynamics and stability characteristics of the observed currents.

Integrating the vertically averaged alongshore velocity along the section, we show with Fig. 10 how the volume transport perpendicular to our section reaches $5.1 \pm 0.24 \text{ Sv}$. Over the shelf and shelfbreak within 50 km of Baffin Island, volume transports are below 0.2 Sv . Seaward of the 800 m isobath, two much larger current structures emerge. The first represents a broad and sluggish flow less than 10 cm/s from about 50 km to 130 km offshore. This flow carries about 1.6 Sv , but a 30 km wide counter-current or eddy structure reduces the net transport to less than 0.8 Sv over the top 500 m of the water column. Most of the volume transport across the Baffin Island section is contained within a southward jet about 160 km from shore near the 2000 m isobath. It alone carries almost 3.5 Sv over its 60 km width from 160 km to 220 km from the coast. The same flow emerges via geostrophy from the hydrographic observations (Figs. 8 and 7). The along-shore velocity within this 60 km wide jet is vertically sheared, so that lateral shear vanishes at 600 m depth, that is, the velocity observed by ADCP at 600 m contributes little to the geostrophic currents that contain both vertical and lateral shear above 300 m. This gives confidence that directly observed ADCP surface currents are consistent with independently estimated geostrophic currents.

4.3. Baffin Island Current Hydrography 1979

We here exploit the finding that the thermal wind relation holds well off Baffin Island by applying it to hydrographic data from the most comprehensive survey conducted along coastal Baffin Island. Fissel et al. (1982) introduce these 1979 data, but focus on the surface circulation off Bylot Island at the entrance to Lancaster Sound just to the north-west of our study area. In Fig. 11 we show 6 across-shore sections from $72^\circ N$ latitude to Davis Strait in the south near $67^\circ N$ latitude, see Fig. 1 for locations. Excluding the northernmost section, geostrophic volume and freshwater flux is towards Davis Strait in the south. Values vary between 1.8 and 4.0 Sv for volume and 78 and 154 mSv for freshwater. Mean values are 3.0 ± 0.9 Sv and 118 ± 35 mSv where the uncertainty is a standard deviation of the along-shore variability. The along-shore continuity is not perfect, but the generally upward sloping isopycnals from about 300 m near the shelf-break to 100 m about 100 km offshore are ubiquitous. This is the cold and fresh outflow from the Canadian Archipelago. The northernmost section with the negative (northward) flux probably does not resolve the offshore extent of the outflow and implies a weak circulation in the lee of Bylot Island. Fissel et al. (1982) report on vigorous eddy activity near the surface at this location which also coincides with our 2003 section revealing less than 0.2 Sv volume flux within 60 km of Baffin Island (Fig. 10). Note also, that 1979 was an NAO-negative year (Figure 13) which implies weaker than average baroclinic circulation. We indeed find the geostrophic thermal wind circulation weaker in 1979 as compared to 2003.

5. Volume and Freshwater Flux

Our two 2003 sections across the shelf, slope, and basin off Greenland and Baffin Island intersect near $73^\circ N$ latitude at the thalweg over the deep Baffin Bay basin (Fig. 1). These sections define a volume that is open to Nares Strait and Jones Sound in the north-east and Lancaster Sound in the north-west. Table 1 summarizes volume and freshwater flux estimates in the form of a closed budget. The net flow into our study area from Nares Strait in the summer of 2003 is about 1.0 ± 0.2 Sv in the absence of winds (Münchow et al., 2007). The West Greenland current systems adds 3.8 ± 0.27 Sv inflow from the south-east. Mooring observations suggest that Jones and Lancaster Sounds can provide an additional 0.3 Sv and 1.0 Sv, respectively. Our control volume thus conserves volume within an uncertainty of 1.0 Sv or about 20% of the outflow. Furthermore, seasonal

cycles are large in Lancaster Sound with volume flux reaching 1.0 Sv in summer and dropping below 0.2 Sv in winter (Peterson et al., 2012).

The situation is similar for freshwater flux q_f which we estimate relative to a salinity $S_0 = 34.8$ psu by integrating observations of salinity $S(x,z)$ and velocity $u(x,z)$ over the sectional area A in the (x,z) plane, e.g., $q_f = \int_A (1 - S/S_0) u dA$. Figs. 3 and 4 show S and u for the West Greenland Current System which provides $q_f = 72 \pm 20$ mSv into our volume. The Baffin Island Current System (Figs. 7 and 9) exports $q_f = 187 \pm 30$ mSv towards Davis Strait. Table 1 summarizes these results and adds estimates for Nares Strait, Lancaster Sound, and Jones Sound. Observations from the summer of 2003 give 34 ± 6 mSv for Nares Strait (Münchow et al., 2007) and 75 ± 10 mSv for Lancaster Sound (Peterson et al., 2012) which balances the freshwater flux within 3% of the outflow, but this is perhaps fortuitous as the uncertainties are an order of magnitude larger (Table 1).

These estimates compare to the net annual mean freshwater flux through Davis Strait of 116 ± 41 mSv for 2004-05 and a mean volume flux of 2.3 ± 0.7 Sv that exit Baffin Bay (Curry et al., 2011). About 1.9 Sv of volume and 27 mSv of freshwater enter Baffin Bay from the south (Curry et al., 2011). Assuming that these Davis Strait inflows to Baffin Bay are contained within our West Greenland section, we conclude that about 1.9 Sv of volume and 27 mSv of freshwater recirculate within northern Baffin Bay. Furthermore, Curry et al. (2011) find that the shelf off West Greenland carries 0.4 Sv in volume and 15 mSv in freshwater flux into Baffin Bay from the south that relate to glacial meltwater (Azetsu-Scott et al., 2012). We thus speculate that most of the observed 2003 circulation over the shelf and slope off north-west Greenland in Baffin Bay is a recirculation of both salty Atlantic and fresher Arctic waters.

6. Climatological Context 1916-2003

1 We start our discussion of the hydrographic climatology of northern Baffin Bay with Fig. 12 which shows the potential temperature on a constant density surface ($\sigma_t = 27.4 \text{ kg m}^{-3}$) derived from the NODC/BIO data as well as our own 2003 data. Zweng and Münchow (2006) discusses the seasonal bias of these data that are generally collected in the summer in ice-free waters. The vertical location of this density surface varies from about 50-m in eastern Davis Strait to more than 350 m depth along Baffin Island. The distribution of potential temperature in Fig. 12 reveals the warm (and thus salty) waters off Greenland exceeding $1^\circ C$ as compared

622 with the cold (and thus less salty) waters off Ellesmere 674
623 and Devon Islands in the north-west with temperatures 675
624 below 0°C . These are the signatures of the West Green- 676
625 land and Baffin Island Currents that together comprise 677
626 the cyclonic circulation. The shallow occurrence of the 678
627 $27.4 \sigma_t$ feature in the center of Baffin Bay near 66°W lon- 679
628 gitude and 72°N latitude is consistent with this cyclonic 680
629 circulation. Note also the patchy temperature distribu- 681
630 tion north of 72°N where the colder, fresher northern wa- 682
631 ters meet the warmer, saltier southern waters. This is an 683
632 area of water mass transition and transformation. 684

633 The temporal context of our detailed 2003 observa- 685
634 tions is demonstrated via the North-Atlantic Oscilla- 686
635 tion (NAO) which represents the dominant mode of at- 687
636 mospheric variability in the northern hemisphere (Hur- 688
637 rell and Deser, 2009). A more deeply depressed Ice- 689
638 landic Low than normal constitutes the positive NAO 690
639 phase. Zweng and Münchow (2006) demonstrate that 691
640 subsurface temperature fluctuations in Baffin Bay corre- 692
641 late significantly with the NAO reflecting Baffin Bay's 693
642 connection to the climate regime of the North-Atlantic. 694
643 Fig. 13 shows the NAO index from 1910 through 2004 695
644 with non-dimensional amplitudes with a range of ± 5 . 696
645 We form conditional averages of hydrographic proper- 697
646 ties for years with NAO amplitudes larger than $+0.5$ and 698
647 smaller than -0.5 . Positive values are associated with 699
648 more intense storms at higher latitudes causing drier and 700
649 colder winter conditions over Greenland and northern 701
650 Canada while negative values are associated with both 702
651 weaker and more southerly storm tracks (Hurrell and 703
652 Deser, 2009). The NAO value for 2003 is $+0.2$, close to 704
653 the average or normal conditions. 705

654 It is instructive to examine how the implied 706
655 geostrophic circulation in Baffin Bay differs between 707
656 positive and negative NAO states. We average the cli- 708
657 matological data into a section across Baffin Bay cre- 709
658 ated by binning observations according to water depth. 710
659 By doing so, we assume that hydrographic properties 711
660 are uniform along isobaths from 67°N to 76°N latitude. 712
661 Depths on the Greenland side have been separately 713
662 binned from those on the Canadian side separated by 714
663 the thalweg - the locus of points at having the greatest 715
664 depth for each latitude. The number of casts entering 716
665 this average varies from a low of 15 in the deep center 717
666 of Baffin Bay to a high of 236 over the slope off West 718
667 Greenland. 719

668 Fig. 14 shows the results of this conditional aver- 720
669 aging in time (separately for high and low NAO years) 721
670 and space (separately east and west of the thalweg by 722
671 bathymetry) for a vertical bin that extends from 200 m 723
672 to 400 m below the surface. This layer likely contains 724
673 elements of both the Baffin Island and the West Green-

land Currents in Baffin Bay. During the positive NAO 674
675 phase this layer is both fresher and cooler off Canada 676
677 in the west and saltier and warmer off Greenland in the 678
679 east relative to the NAO negative phase. This indicates a 680
681 stronger (weaker) than normal cyclonic circulation dur- 682
683 ing the NAO positive (negative) phases consistent with 684
685 the earlier findings of Smith (1931) that more (less) 686
687 icebergs occur off Newfoundland during years with a 688
689 positive (negative) NAO anomaly, because it implies 690
691 enhanced southward flux of cold, fresh Arctic waters 692
693 along Canada and enhanced northward flux of warmer, 694
695 saltier Atlantic waters along West Greenland. 696

697 The depth of isopycnals across Baffin Bay increase 698
699 from west to east in all years. This indicates a net baro- 700
701 clinic outflow from the Arctic into the North-Atlantic 702
703 Ocean relative to zero flow below. Nevertheless, there 704
705 are smaller baroclinic features confined to the conti- 706
707 nental slope ($1500\text{-}2000\text{ m}$ isobaths) that demarcate the 708
709 shelf from the deep basin off Baffin Island. Specific- 710
711 ally during negative NAO years, the density anomaly 711
712 σ_t varies by only 0.03 kg m^{-3} ($27.32\text{-}27.35\text{ kg m}^{-3}$), but 713
714 during positive NAO years σ_t varies across the shelf 715
716 break by more than 0.09 kg m^{-3} ($27.28\text{-}27.35\text{ kg m}^{-3}$). 717
718 We speculate that the waters above the $1500\text{-}2000\text{ m}$ 719
720 isobath at $200\text{-}400\text{ m}$ depth are part of the climatologi- 721
722 cal Baffin Island Current. 723

724 Density at fixed depth increases between the 1500- 725
726 m isobath and the coast of Baffin Island on the Cana- 727
728 dian side. The size of the increase is greater within 729
730 the domain centred at 200-m depth than that centred 731
732 at 300 m (Fig. 14 and 15). If the lateral density gra- 733
734 dients are geostrophically balanced relative to a deeper 734
735 level without flow, then this gradient implies a possi- 736
737 ble northward counter-current in shallow water that has 737
738 also been noted by Tang et al. (2004) and Curry et al. 738
739 (2011). The same geostrophic shear could also be facil- 739
740 itated by a subsurface flow that has a southward max- 740
741 imum at depth. A velocity section across Nares Strait 741
742 shows such enhanced subsurface jet in geostrophic ther- 742
743 mal balance (Münchow et al., 2007). 743

744 Identical results emerge for a smaller vertical inter- 745
746 val closer to the surface: Figure 15 shows condition- 746
747 ally averages properties between 150 m and 250 m be- 747
748 low the surface. This layer emphasizes the shallower 748
749 Baffin Island Current over the deeper West Greenland 749
750 Slope Current. The northward countercurrent off Baffin 750
751 Island appears stronger in the $150\text{-}250\text{ m}$ as compared 751
752 to the $200\text{-}400\text{ m}$ averages for both positive and nega- 752
753 tive NAO states. Despite these details, the conditional 753
754 averaging by NAO along isobath reveals robust features 754
755 of the mass and heat distribution within Baffin Bay that 755
756 do not depend on the details of the vertical averaging or 756

726 NAO cut-off.

727 7. Discussion

728 Analyses of hydrographic data in Baffin Bay during
729 the 1916-2003 period indicate that the NAO index mod-
730 ulates the baroclinic pressure distribution inside Baffin
731 Bay (Figs. 14 and 15), creating a stronger geostrophic
732 cyclonic circulation during the NAO-positive years such
733 as 1919, 1973, 1984, and 1990 than it is during the
734 NAO-negative years such as 1916, 1936, 1969, and
735 1996 (Fig. 13). These finding also demonstrates
736 why differencing hydrographic properties from the early
737 1960's from those of the 1990's reveals large signals,
738 e.g., Dickson et al. (2003) and Dickson et al. (2002).
739 During this period the NAO goes from an extreme neg-
740 ative to an extreme positive state with attendant large
741 variations in circulation. Only long-term records cov-
742 ering a full cycle of such oscillations will provide the
743 data to distinguish such climate oscillations from the
744 more steady man-made globally warming signals ob-
745 served in the atmosphere (Ring et al., 2012). Zweng
746 and Münchow (2006) demonstrate that these warming
747 signals reach into Baffin Bay at 600 m depth. Inside
748 Baffin Bay they promote subsurface melting of tidewat-
749 er glaciers along West Greenland (Holland et al., 2008).

750 Surface waters off Baffin Island are fresher and colder
751 during NAO-positive years while those off Greenland
752 are saltier and warmer. This finding is consistent with
753 a more energetic circulation in Baffin Bay. Zweng and
754 Münchow (2006) demonstrate that the warming of sub-
755 surface waters in Baffin Bay correlates significantly
756 with the NAO which emphasizes the connection of the
757 regional oceanography with remote atmospheric forcing
758 over the North-Atlantic at interannual time scales. We
759 consider our 2003 observations to represent a climato-
760 logical mean rather than an extreme state, because the
761 NAO index was close to zero in both 2002 and 2003.

762 During our summer 2003 survey of northern Baffin
763 Bay we find a delicate spatial arrangements of water
764 masses and ocean currents within about 600 m of the
765 surface. The waters off western Greenland are strongly
766 impacted by relatively warm and salty waters originat-
767 ing from the North-Atlantic entering via Davis Strait
768 (Cuny et al., 2005; Tang et al., 2004) while those off
769 Baffin Island are strongly impacted by relatively cold
770 and fresh waters originating from the Arctic Ocean
771 (Münchow and Melling, 2008; Prinsenberg and Hamil-
772 ton, 2005; Peterson et al., 2012). Waters are strongly
773 stratified in the vertical both off West Greenland in the
774 east and off Baffin Island in the west. In contrast, lat-
775 eral density gradients over the slope off Greenland are

776 small relative to those found off Baffin Island and im-
777 ply a weak baroclinic circulation in geostrophic (ther-
778 mal wind) balance.

779 Weak baroclinic circulation does not imply weak
780 flows, however, because the total flow also contains a
781 barotropic component. Specifically, we find a 20 km
782 wide, largely barotropic flow centered over the 600 m
783 isobath west of Greenland. This flow, which we call
784 the West Greenland Slope Current, carries about 2 Sv
785 ($10\text{ m}^6\text{s}^{-1}$) towards the north-west during our survey. It
786 contains the warmest waters found in northern Baffin
787 Bay with potential temperatures exceeding $2\text{ }^\circ\text{C}$ at 400
788 m below the surface in 600 m deep water. This slope
789 current is distinct from the flows both seaward over the
790 deep basin and landward over the the continental shelf.

791 Flows off Baffin Island are largely in baroclinic
792 geostrophic balance as evidenced by directly measured
793 ocean currents (Figs. 8 and 9). Both velocity observa-
794 tions and geostrophic diagnostics reveal the main cir-
795 culation features over the sloping topography off Baffin
796 Island, namely (1) a slow broad southward flow within
797 about 150 km of the coast and (2) an intense, surface in-
798 tensified cyclonic feature with southward velocities ex-
799 ceeding 0.4 m s^{-1} within 15 km of a weaker, but north-
800 ward surface velocity core reaching 0.2 m s^{-1} . The
801 broad sluggish inshore flow carries about 1 Sv while the
802 50 km wide offshore feature carries another 4.4 Sv of
803 volume southward. The latter is centered near the 2000
804 m isobath about 180 km from the coast of Baffin Island.
805 It coincides with isopycnals that slope by about 100 m
806 over 20 km almost uniformly from 450 m to 50 m depth.
807 Comparing the direct velocity observations with those
808 estimated from hydrography via the geostrophic thermal
809 wind relation, we conclude that the vertical shear mea-
810 sured by the vessel-mounted ADCP off Baffin Island is
811 largely geostrophic and baroclinic.

812 Seaward of the West Greenland Slope Current we
813 identify anomalous waters that extend from the surface
814 to about 800 m depth within an anti-cyclonic circula-
815 tion feature that is well modeled as a Rankine vortex
816 with a diameter of about 10 km (Fig. 5). The small 10-
817 km scale of this eddy corresponds to the internal (baro-
818 clinic) Rossby radius of deformation which is the dom-
819 inant spatial scale for a stratified fluid in geostrophic
820 balance (Gill, 1982), however, it also corresponds to
821 the width of the continental slope and the width of the
822 barotropic West Greenland Slope Current. The anti-
823 cyclonic eddy extends across the entire halocline with
824 a thickness exceeding 400 m near continental slope
825 where most of the kinetic energy is contained within the
826 largely barotropic West Greenland Slope Current. It re-
827 circulates a volume flux of about $0.8 \pm 0.2\text{ Sv}$.

828 A single CTD cast from the core of the vortex dis- 880
829 tinctly separates temperature-salinity correlation curves 881
830 from a grouping representative of West Greenland shelf 882
831 waters off Cape York and a grouping representative of 883
832 Baffin Bay basin waters with salinities above 33.5 psu 884
833 (Figs. 2 and 6). Specifically, above salinities of 33.5 885
834 psu, the entire salinity-temperature correlation falls be- 886
835 tween the shelf and basin cluster of CTD profiles. Water
836 temperatures within the vortex are about 0.2 °C warmer
837 than than slope and basin waters and 0.4°C cooler than
838 shelf waters on the same isopycnals. The northward
839 flow of Atlantic waters via Davis Strait is the source
840 of the waters over the slope (Tang et al., 2004). This
841 inflow is seasonally modulated in both its velocity mag-
842 nitude (Cuny et al., 2005), its subsurface temperature
843 maximum (Zweng and Münchow, 2006), and its heat
844 transport into Baffin Bay. Davis Strait is about 800 km
845 to the south. Assuming a swift flow over the slope of 0.2
846 $m s^{-1}$, a water parcel would arrive at our study region
847 about 45 days later. We thus speculate that the eddy rep-
848 represents hydrographic conditions of the West Greenland
849 Slope Current at least 2 months prior.

850 A definite explanation for the origin of this anti-
851 cyclonic circulation feature requires more comprehen-
852 sive observations and numerical modeling. Katsman
853 et al. (2004) and Spall et al. (2008) discuss eddy dy-
854 namics related to slope and boundary currents in nu-
855 merical models to explain observations off south-west
856 Greenland and north-west Alaska, respectively. Both
857 these studies identify baroclinic instability as the main
858 eddy formation process, however, our limited observa-
859 tions indicate that most of the kinetic energy over the
860 slope off West Greenland is barotropic. The scale of
861 the vortex is of the same order of magnitude as both
862 the width of the slope and the internal deformation ra-
863 dius. Hence we are presently unsure which instabil-
864 ity process generated the anti-cyclonic eddy seaward of
865 the West Greenland Slope Current. We do note, how-
866 ever, that the barotropic circulation over the continental
867 slope off West Greenland resembles the West Spitsber-
868 gen Current in the Greenland Sea (Walczowski et al.,
869 2005) which is postulated to become barotropically un-
870 stable (Teigen et al., 2010).

871 It is unclear, however, how a barotropic circulation
872 over the steeply sloping shelf break off West Green-
873 land transforms into a baroclinic circulation largely de-
874 tached from the bottom over much deeper water off Baf-
875 fin Island. Within about 150 km off Baffin Island the
876 circulation is sluggish during our observations in July
877 2003, however, we find largest currents as a single sur-
878 face intensified, 50-km wide baroclinic jet about 180
879 km from the coast. Vertical currents shears predicted

from geostrophy agree well with vertical shears mea-
sured from vessel-mounted ADCP surveys. Counter-
currents or eddies appear in the velocity section (Fig.
9) that correspond to sloping and undulating isopycnals
in apparent geostrophic balance. Lateral current shears
suggest Rossby numbers of up to 0.25 or a weakly non-
linear flow off Baffin Island.

887 8. Conclusions

888 Direct velocity observations from vessel-mounted
889 ADCP reveal that the circulation off both West Green-
890 land and Baffin Island contains multiple velocity cores,
891 eddies, and counter-currents at scales that correspond
892 to both the internal Rossby radius of deformation and
893 topographic slopes. Most of these flow features corre-
894 late well with distinct water mass properties that sug-
895 gest geostrophic dynamics. More intense flows over
896 the slope off West Greenland implicate nonlinear inert-
897 ial forces as Rossby numbers reach 0.4 within an anti-
898 cyclonic eddy that is well represented as a Rankine vor-
899 tex.

900 The outflow of cold and fresh Arctic waters from
901 Nares Strait and Lancaster Sound transforms into the
902 Baffin Island Current with substantial contributions
903 from the warmer and saltier Atlantic waters of the West
904 Greenland Current system. Comparing directly mea-
905 sured current shears to those estimated from hydro-
906 graphic observations in 2003, we find the Baffin Island
907 Current, but not the West Greenland Current system in
908 geostrophic thermal wind balance. Hydrographic ob-
909 servations alone thus will not provide accurate velocity
910 or flux estimates over the slope off West Greenland on
911 account of a strong barotropic flow. We thus conclude
912 that direct velocity measurements are needed to describe
913 current off western Greenland.

914 Analysis of almost 100 years of historical hydro-
915 graphic (summer) data indicates that our 2003 observa-
916 tions are close to a climatological mean state as defined
917 by the NAO. Conditional averaging along isobaths re-
918 veals a more intense baroclinic counter-clockwise cir-
919 culation in Baffin Bay during positive NAO years as
920 compared to years with negative NAO. This is consis-
921 tent with earlier findings by Smith (1931) of larger ice-
922 berg counts off Labrador and Newfoundland during pos-
923 itive NAO years. It is also consistent with recent mod-
924 eling work of the Arctic Ocean that the freshwater ac-
925 cumulated within the Beaufort gyre (Proshutinsky et al.,
926 2009) is released into the Atlantic preferentially during
927 years with positive NAO (Haine, 2013, pers. comm.).

928 **9. Acknowledgments**

929 The National Science Foundation supported the ini-
930 tial fieldwork with Grant 0230236 (AM and HM),
931 0230354 (KKF) while the analyses were supported by
932 1022843 (AM). The Canadian Department of Fisheries
933 and Oceans and University of Delaware supported this
934 study with salaries, institutional, and logistical infras-
935 tructure.

References

Addison, V.G., 1987. Physical oceanography of the northern Baffin Bay - Nares Strait region. Master's thesis. Monterey, CA, 110pp.

Azetsu-Scott, K., Petrie, B., Yeats, P., Lee, C., 2012. Composition and fluxes of freshwater through Davis Strait using multiple chemical tracers. *J. Geophys. Res.* 117, C12011.

Bacle, J., Carmack, E.C., Ingram, R.G., 2002. Water column structure and circulation under the North Water during spring transition: April-july 1998. *Deep-Sea Res.* 49, 4907-4925.

Bacon, S., Reverdin, G., Rigor, I.G., Snaith, H.M., 2002. A freshwater jet on the East Greenland shelf. *J. Geophys. Res.* 107, 3068.

Berton, P., 1988. *The Arctic Grail*. Viking Penguin Inc., New York, NY, 672pp.

Bourke, R.H., Addison, V.G., Paquette, R.G., 1989. Oceanography of Nares Strait and northern Baffin-Bay in 1986 with emphasis on deep and bottom water formation. *J. Geophys. Res.* 94, 8289-8302.

Cuny, J., Rhines, P.B., Kwok, R., 2005. Davis Strait volume, freshwater and heat fluxes. *Deep-Sea Res.* 52, 519-542.

Curry, B., Lee, C.M., Petrie, B., 2011. Volume, freshwater, and heat fluxes through davis strait, 2004-05. *J. Phys. Oceanogr.* 41, 429-436.

Dickson, B., Yashayaev, I., Meincke, J., Turrell, B., Dye, S., Holfort, J., 2002. Rapid freshening of the deep North Atlantic Ocean over the past four decades. *Nature* 416, 832-837.

Dickson, R.R., Curry, R., Yashayaev, I., 2003. Recent changes in the North Atlantic. *Phil. Trans. R. Soc. Lond. Series A* 361, 1917-1933.

Dumont, D., Gratton, Y., Arbetter, T.E., 2009. Modeling the dynamics of the North Water polynya ice bridge. *J. Phys. Oceanogr.* 39, 1448-1461.

Dunbar, M., 1951. Eastern arctic waters. *Bull. Fish. Res. Board Can.* 88, 1-131.

Fissel, D.B., Lemon, D.D., Birch, J.R., 1982. Major features of the summer near-surface circulation of western Baffin-Bay, 1978 and 1979. *Arctic* 35, 180-200.

Francis, J.A., Vavrus, S.J., 2012. Evidence linking Arctic amplification to extreme weather in mid-latitudes. *Geophys. Res. Lett.* 39, L06801.

Gill, A., 1982. *Atmosphere-Ocean Dynamics*. Academic Press Inc.

Greene, C., Pershing, J., Cronin, T., Ceci, N., 2008. Arctic climate change and its impacts on the ecology of the North Atlantic. *Ecology* 89 Suppl., S24-S38.

Holland, D.M., Thomas, R.H., De Young, B., Ribergaard, M.H., Lyberth, B., 2008. Acceleration of Jakobshavn Isbrae triggered by warm subsurface ocean waters. *Nature Geoscience* 1, 659-664.

Hurrell, J.W., Deser, C., 2009. North Atlantic climate variability: The role of the North Atlantic Oscillation. *J. Mar. Sys.* 78, 28 - 41.

Ingram, R.G., Bacle, J., Barber, D.G., Gratton, Y., Melling, H., 2002. An overview of physical processes in the North Water. *Deep-Sea Res.* 49, 4893-4906.

Katsman, C.A., Spall, M.A., Pickart, R.S., 2004. Boundary current eddies and their role in the restratification of the Labrador Sea. *J. Phys. Oceanogr.* 34, 1967-1983.

Kiilerich, A., 1939. The Godthaab Expedition 1928 - a theoretical treatment of the hydrographic observation material. *Meddeleser Gronland* 78, 1-148.

Kwok, R., Rothrock, D.A., 2009. Decline in Arctic sea ice thickness from submarine and icesat records: 1958-2008. *Geophys. Res. Lett.* 36, L15501-.

LeBlond, P.H., 1980. On the surface circulation in some channels of the Canadian Arctic Archipelago. *Arctic* 33, 189-197.

Lin, N., Emanuel, K., Oppenheimer, M., Vanmarcke, E., 2012. Physically based assessment of hurricane surge threat under climate change. *Nature Climate Change* 2, 462-467.

Melling, H., 2000. Exchange of freshwater transport through the shallow straits of the North American Arctic. Kluwer Academic Publishers, Dordrecht, Netherlands. chapter 20. pp. 479-502.

Melling, H., Agnew, T., Falkner, K., Greenberg, D., Lee, C., Münchow, A., Petri, B., Prinsenberg, S., Samelson, R., Woodgate, R., 2008. Fresh-water fluxes via Pacific and Arctic outflows across the Canadian polar shelf. Springer Verlag, Dordrecht, Netherlands. chapter 9. pp. 193-261.

Muench, R., 1971. The physical oceanography of the northern Baffin Bay region. Technical Report. Baffin Bay - North Water Scientific Report No. 1.

Münchow, A., 2000. Detiding three-dimensional velocity survey data in coastal waters. *J. Atmos. Oceanic Technol.* 17, 736-748.

Münchow, A., Falkner, K., Melling, H., 2007. Spatial continuity of measured seawater and tracer fluxes through Nares Strait, a dynamically wide channel bordering the Canadian Archipelago. *J. Mar. Res.* 65 (6), 759-788.

Münchow, A., Garvine, R.W., 1993. Dynamical properties of a buoyancy-driven coastal current. *J. Geophys. Res.* 98, 20063-20077.

Münchow, A., Melling, H., 2008. Ocean current observations from Nares Strait to the west of Greenland: Interannual to tidal variability and forcing. *J. Mar. Res.* 66 (6), 801-833.

Münchow, A., Melling, H., Falkner, K.K., 2006. An observational estimate of volume and freshwater flux leaving the Arctic Ocean through Nares Strait. *J. Phys. Oceanogr.* 36, 2025-2041.

Padman, L., Erofeeva, S., 2004. A barotropic inverse tidal model for the Arctic Ocean. *Geophys. Res. Lett.* 31, L02303.

Peterson, I., Hamilton, J., Prinsenberg, S., Pettipas, R., 2012. Wind-forcing of volume transport through Lancaster Sound. *J. Geophys. Res.* 117, C11018.

Pimenta, F., Garvine, R.W., Münchow, A., 2008. Observations of coastal upwelling off Uruguay downshelf of the Plata estuary, South America. *J. Mar. Res.* 66, 835-872.

Prinsenberg, S.J., Hamilton, J., 2005. Monitoring the volume, freshwater and heat fluxes passing through Lancaster Sound in the Canadian Arctic Archipelago. *Atmos.-Oceans* 43, 1-22.

Proshutinsky, A., Krishfield, R., Timmermans, M.L., Toole, J., Carmack, E., McLaughlin, F., Williams, W.J., Zimmermann, S., Itoh, M., Shimada, K., 2009. Beaufort Gyre freshwater reservoir: State and variability from observations. *J. Geophys. Res.* 114, C00A10.

Rabe, B., Johnson, H., Münchow, A., Melling, H., 2012. Geostrophic currents and freshwater fluxes through Nares Strait to the west of northern Greenland. *J. Mar. Res.* 70, 603-640.

Ring, M., Lindner, D., Cross, E., Schlesinger, M., 2012. Causes of the global warming observed since the 19th century. *Atmospheric and Climate Sciences* 2 (4), 401-415.

Rudels, B., 2011. Volume and freshwater transports through the Canadian Arctic Archipelago-Baffin Bay system. *J. Geophys. Res.* 116, C00D10.

Sallenger, A.H., Doran, K.S., Howd, P.A., 2012. Hotspot of accel-

- ated sea-level rise on the Atlantic coast of North America. *Nature Clim. Change* 2, 884–888.
- Serreze, M.C., Barrett, A.P., Slater, A.G., Woodgate, R.A., Aagaard, K., Lammers, R.B., Steele, M., Moritz, R., Meredith, M., Lee, C.M., 2006. The large-scale freshwater cycle of the Arctic. *J. Geophys. Res.* 111, C11010.
- Shepherd, A., Ivins, E.R., Geruo, A., Barletta, V.R., Bentley, M.J., Bettadpur, S., Briggs, K.H., Bromwich, D.H., Forsberg, R., Galin, N., Horwath, M., Jacobs, S., Joughin, I., King, M.A., Lenaerts, J.T.M., Li, J.L., Ligtenberg, S.R.M., Luckman, A., Luthcke, S.B., McMillan, M., Meister, R., Milne, G., Mouginot, J., Muir, A., Nicolas, J.P., Paden, J., Payne, A.J., Pritchard, H., Rignot, E., Rott, H., Sorensen, L.S., Scambos, T.A., Scheuchl, B., Schrama, E.J.O., Smith, B., Sundal, A.V., van Angelen, J.H., van de Berg, W.J., van den Broeke, M.R., Vaughan, D.G., Velicogna, I., Wahr, J., Whitehouse, P.L., Wingham, D.J., Yi, D.H., Young, D., Zwally, H.J., 2012. A reconciled estimate of ice-sheet mass balance. *Science* 338, 1183–1189.
- Smith, E., 1931. The Marion expedition to Davis Strait and Baffin Bay, Scientific results, part 3. 19, United States Government Printing Office, Washington, DC.
- Spall, M.A., Pickart, R.S., Fratantoni, P.S., Plueddemann, A.J., 2008. Western Arctic shelfbreak eddies: Formation and transport. *J. Phys. Oceanogr.* 38, 1644–1668.
- Sutherland, D.A., Pickart, R.S., 2008. The East Greenland Coastal Current: Structure, variability, and forcing. *Progr. Oceanogr.* 78, 58–77.
- Sutherland, D.A., Pickart, R.S., Jones, E.P., Azetsu-Scott, K., Eert, A.J., Olafsson, J., 2009. Freshwater composition of the waters off southeast Greenland and their link to the Arctic Ocean. *J. Geophys. Res.* 114, C05020.
- Tang, C.C.L., Ross, C.K., Yao, T., Petrie, B., DeTracey, B.M., Dunlap, E., 2004. The circulation, water masses and sea-ice of Baffin Bay. *Progr. Oceanogr.* 63, 183–228.
- Teigen, S., Nilsen, F., Gjevik, B., 2010. Barotropic instability in the West Spitsbergen Current. *J. Geophys. Res.* 115, C07016.
- Timmermans, M.L., Toole, J., Proshutinsky, A., Krishfield, R., Plueddemann, A., 2008. Eddies in the Canada Basin, Arctic Ocean, observed from ice-tethered profilers. *J. Phys. Oceanogr.* 38, 133–145.
- Walczowski, W., Piechura, J., Osinski, R., Wiczorek, P., 2005. The West Spitzbergen Current volume and heat transport from synoptic observations in summer. *Deep-Sea Res.* 52, 1374–1391.
- Woodgate, R.A., Aagaard, K., 2005. Revising the Bering Strait freshwater flux into the Arctic Ocean. *Geophys. Res. Lett.* 32, L02602.
- Zweng, M.M., Münchow, A., 2006. Warming and freshening of Baffin Bay, 1916–2003. *J. Geophys. Res.* 111, C07016.

Table 1: Flux estimates for 2003 surveys of northern Baffin Bay and published mooring data, e.g., Peterson et al. (2012) for Lancaster and Melling (2000) for Jones Sounds. Positive (negative) sign indicates flux into (out of) a closed volume.

Section	Volume (Sv)	Freshwater (mSv)	Source
West Greenland	3.8 ± 0.3	72 ± 20	Survey
Nares Strait	1.0 ± 0.2	34 ± 6	Survey
Baffin Island	-5.1 ± 0.2	-187 ± 30	Survey
Lancaster Sound	1.0 ± 0.2	75 ± 10	Moorings
Jones Sound	0.3 ± 0.1	unknown	Moorings
Sum	1.0 ± 1.0	-6 ± 66	

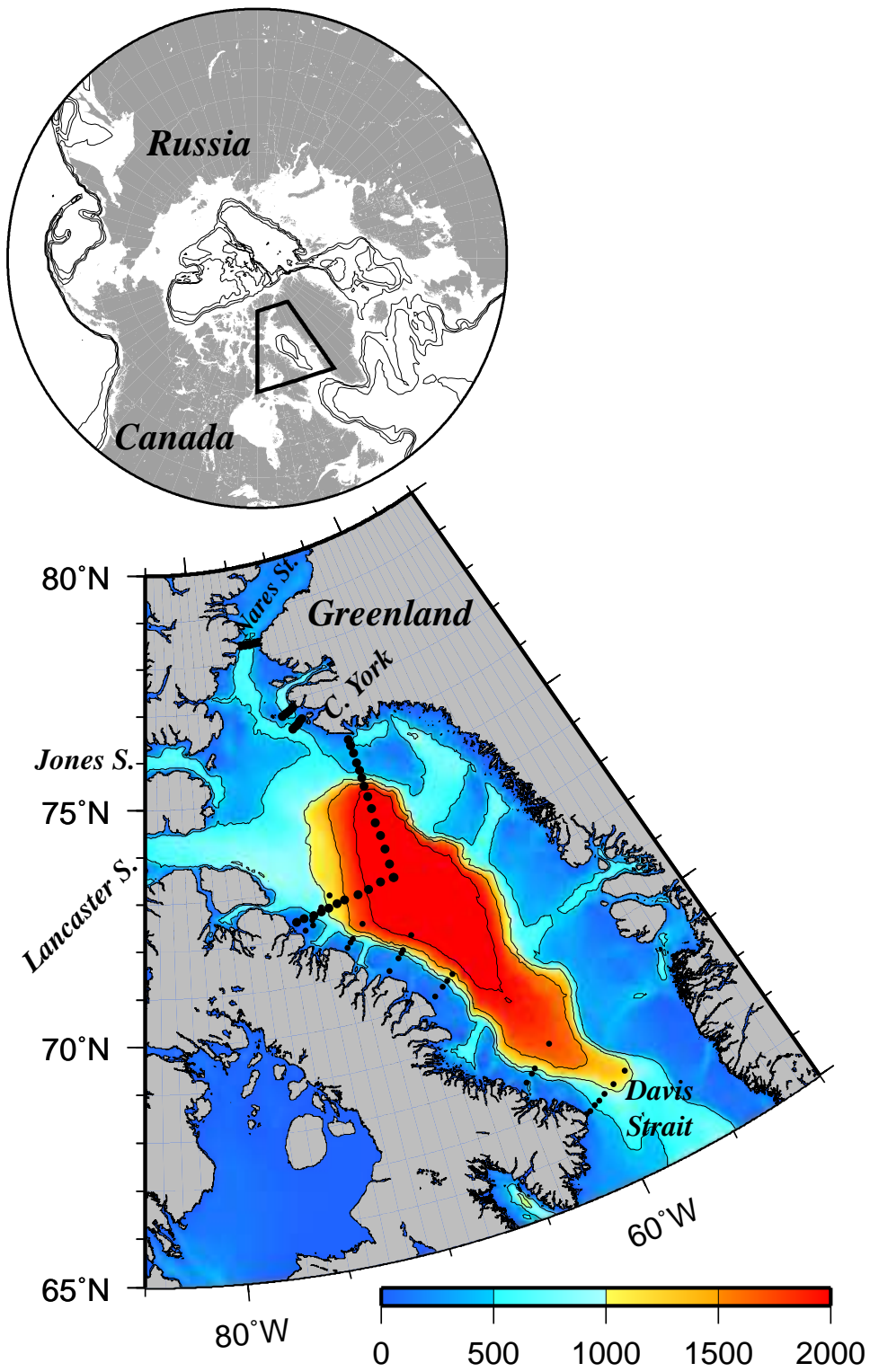


Figure 1: Map of the study area over topography along with CTD station locations in northern Baffin bay for 2003 (large circles) and along Baffin Island for 1979 (small circles).

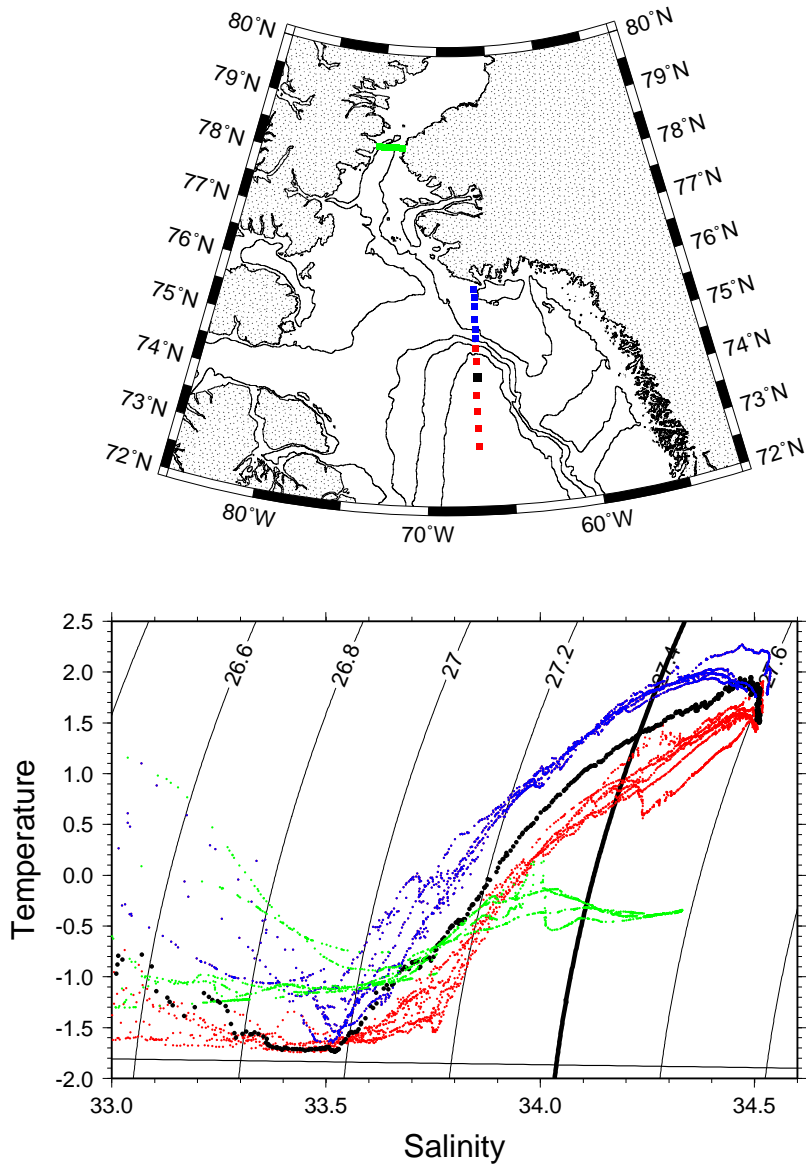


Figure 2: CTD station locations over 500-m, 1000-m, 1500-m, and 2000-m contours of bottom depth (top) and potential temperature ($^{\circ}C$) salinity (in psu) correlations above 600 m over contours of density (bottom). The 27.4 kg m^{-3} contour is highlighted as temperatures on this isopycnal demonstrate the influence of Arctic and Atlantic waters). Colors represent locations and properties of different physical domains (see text for details).

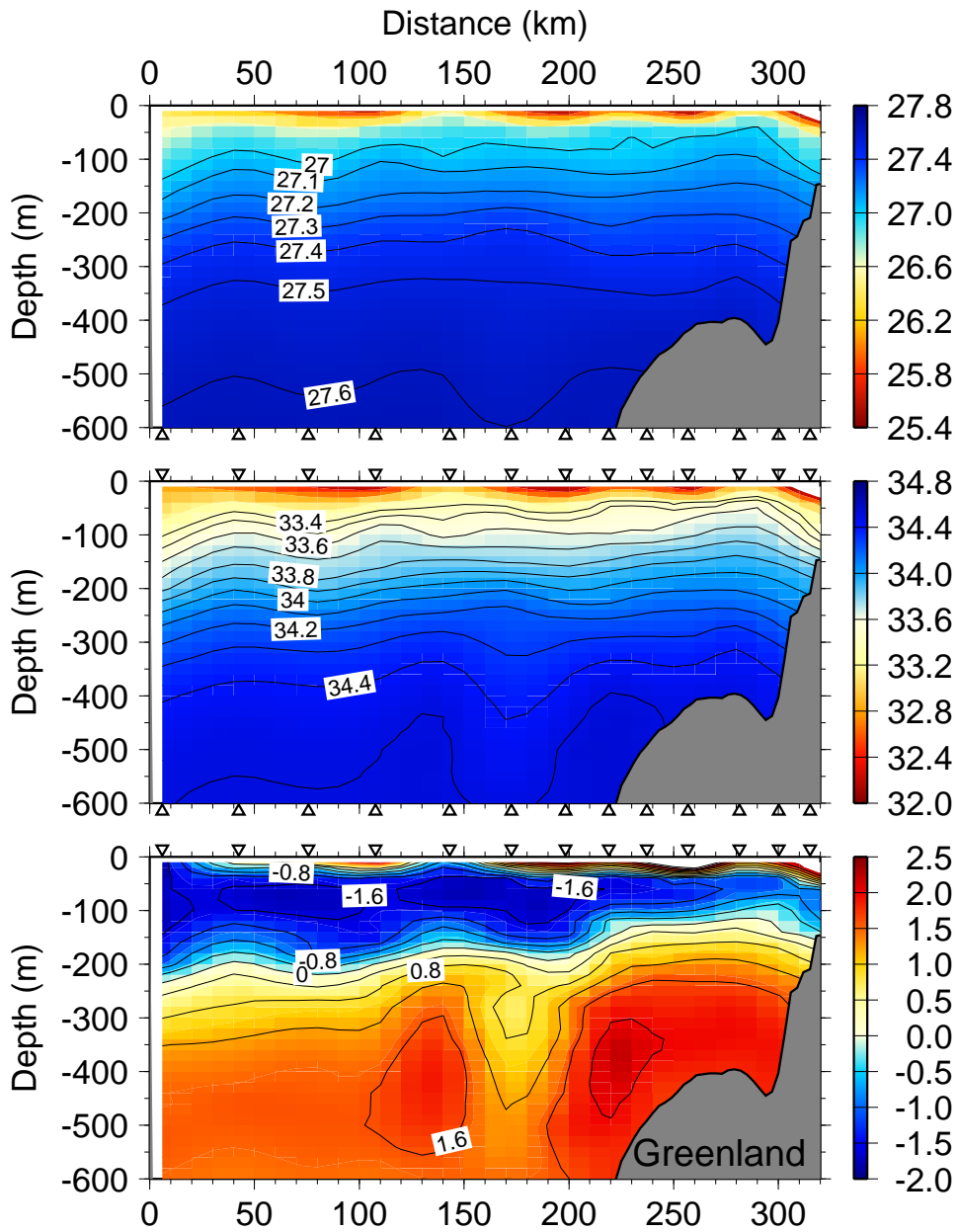


Figure 3: Section off Cape York, Greenland, July 30/31, 2003 for density anomaly σ_t (top panel), salinity (middle panel), and potential temperature (bottom panel). Station locations are indicated by triangles.

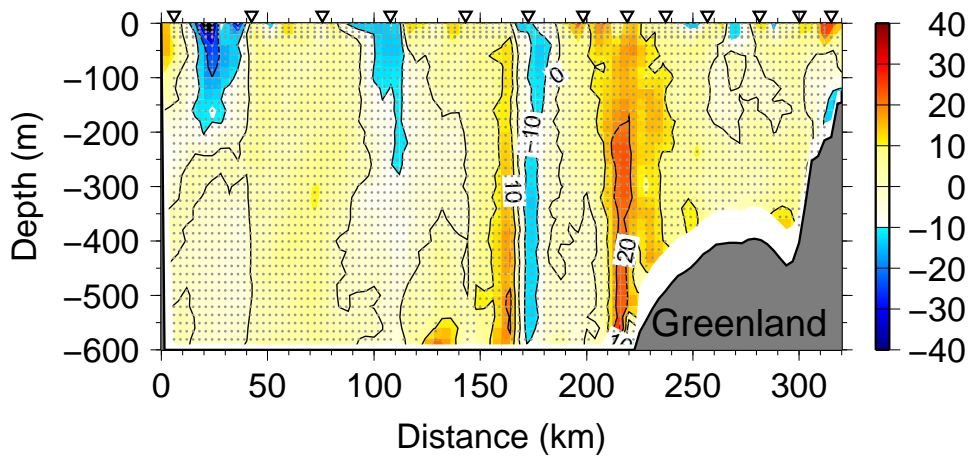


Figure 4: Velocity section off Cape York, Greenland, July 30/31, 2003 from ship-based ADCP surveys. Large inverted triangles indicate CTD station locations to ease comparison with Fig. 3. Small symbols indicate locations of velocity measurements.

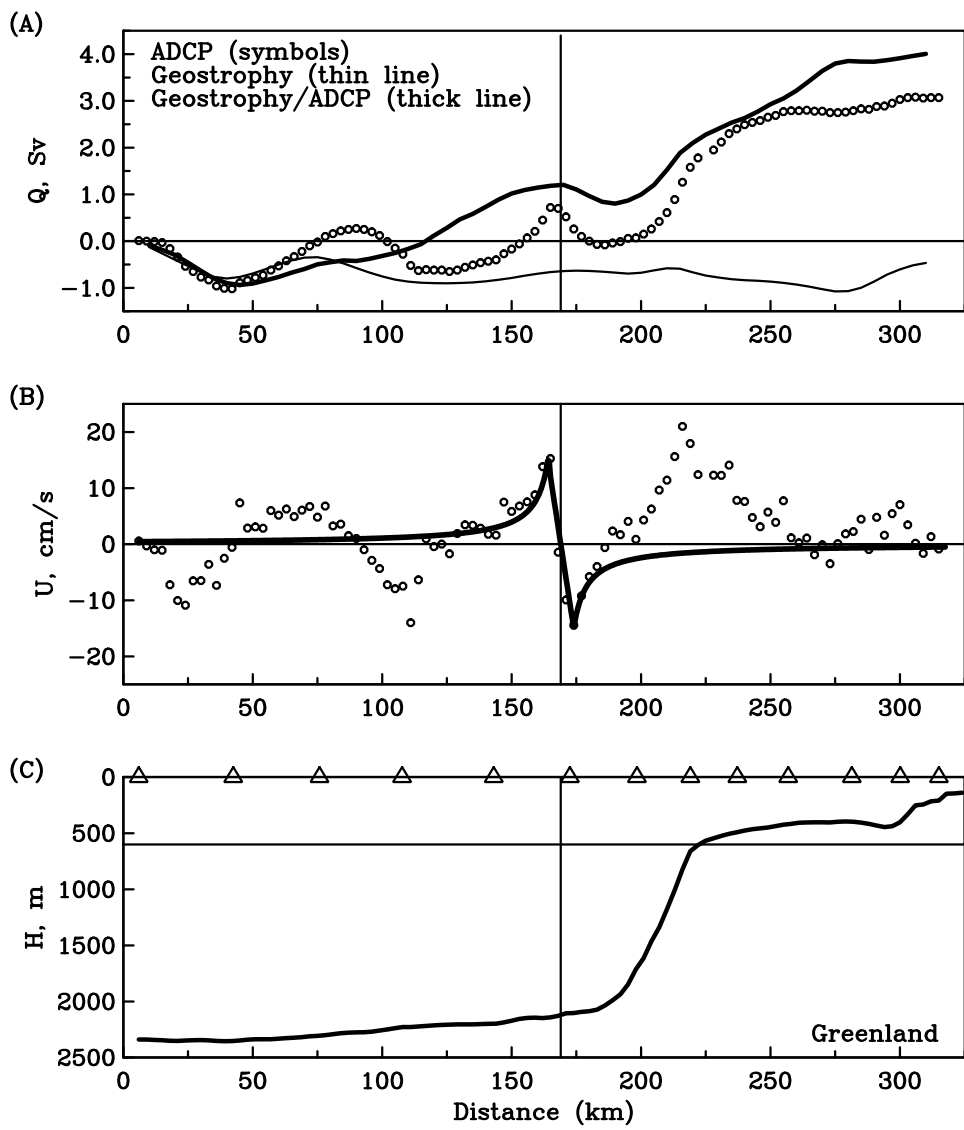


Figure 5: Cape York section, Greenland, July 30/31, 2003: (a) cumulative volume flux over top 600 m from ADCP (symbols) and thermal wind relative to zero flow at bottom or 600-m (thin line) or relative to bottom ADCP (thick line); (b) vertically averaged along-shore ADCP velocity component (symbols) with Rankine vortex profile (line), and (c) bottom topography. The vertical line in each panel indicate the center of the Rankine vortex, symbol indicate CTD station locations, e.g., Fig. 3.

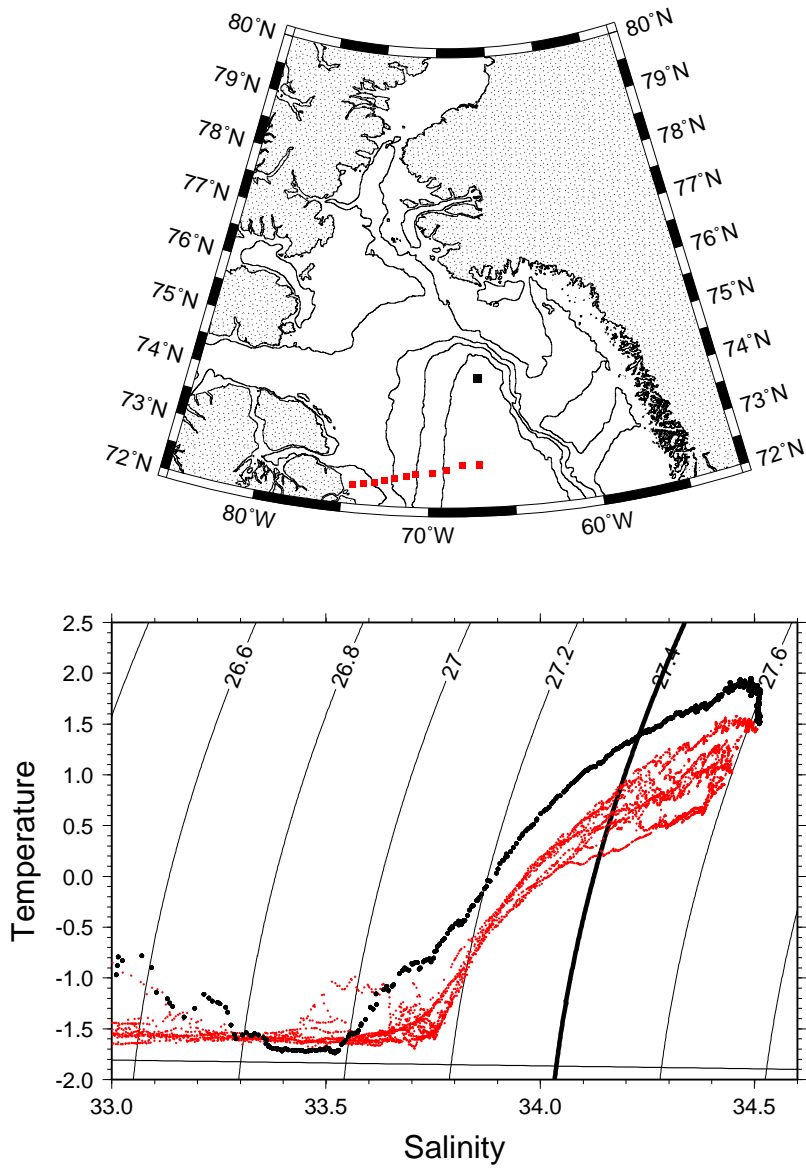


Figure 6: CTD station locations over contours of bottom depth from 500 m to 2000 m (top) and potential temperature salinity correlations above 600 m over contours of density (bottom). The 1027.4 kg m^{-3} contour is highlighted as temperatures on this isopycnal demonstrate the influence of Arctic and Atlantic waters (see Fig. 12). Bold black symbols indicate a cast that is also shown in Fig. 2 for comparison.

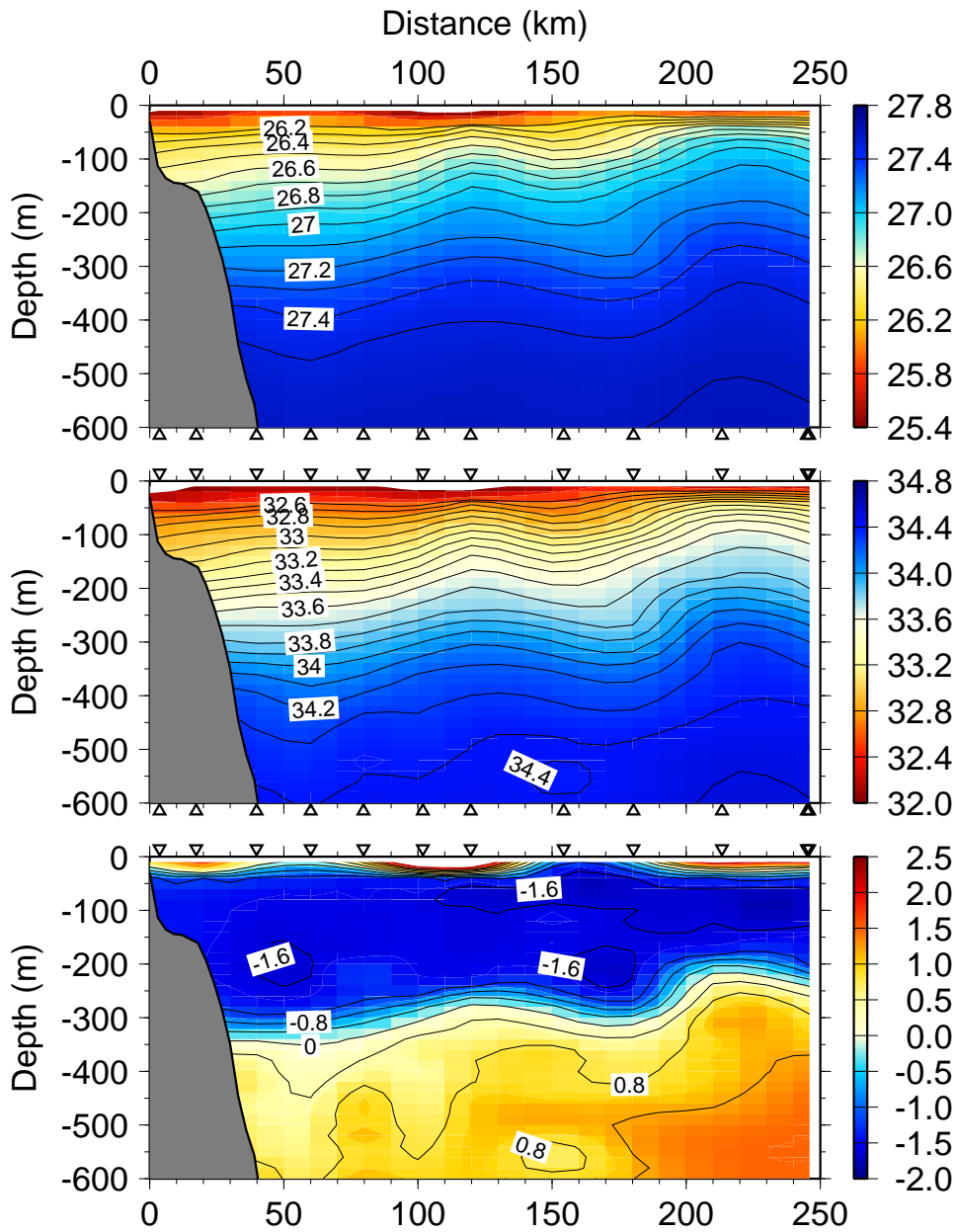


Figure 7: Section off Baffin Island, Canada, July 26/27, 2003 for density anomaly σ_t (top panel), salinity (middle panel), and potential temperature (bottom panel). Station locations are indicated by triangles.

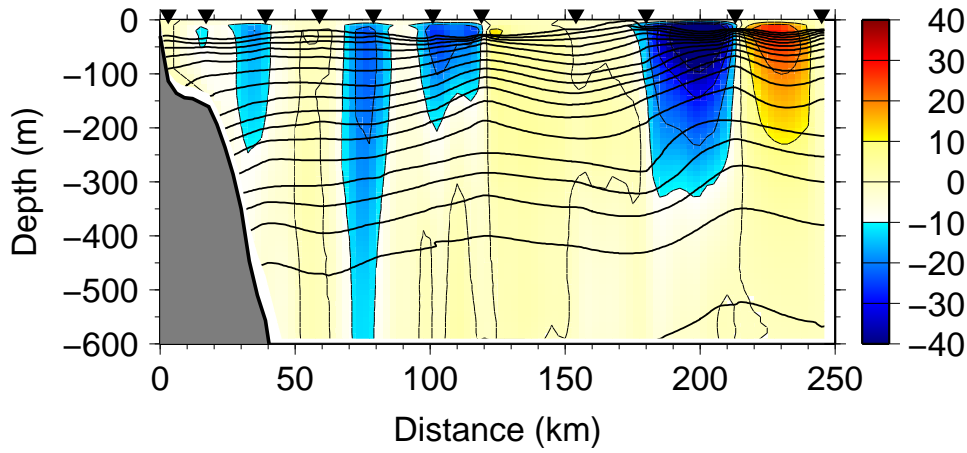


Figure 8: Velocity section off Baffin Island as predicted from the thermal wind relation, July 26/27, 2003 relative to measured ADCP flow at the bottom or 600 m depth. Contours are those of density (Fig. 7) from CTD casts whose location is shown as triangles.

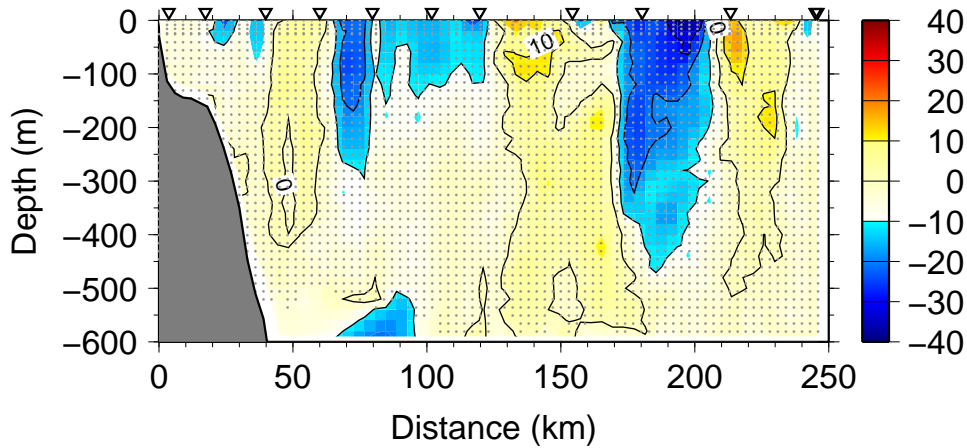


Figure 9: Velocity section off Baffin Island, Canada, July 26/27, 2003 as measured by vessel-mounted ADCP. Triangles indicate CTD locations, small symbols indicate ADCP measurement locations averaged into 3-km wide and 15 m deep bins.

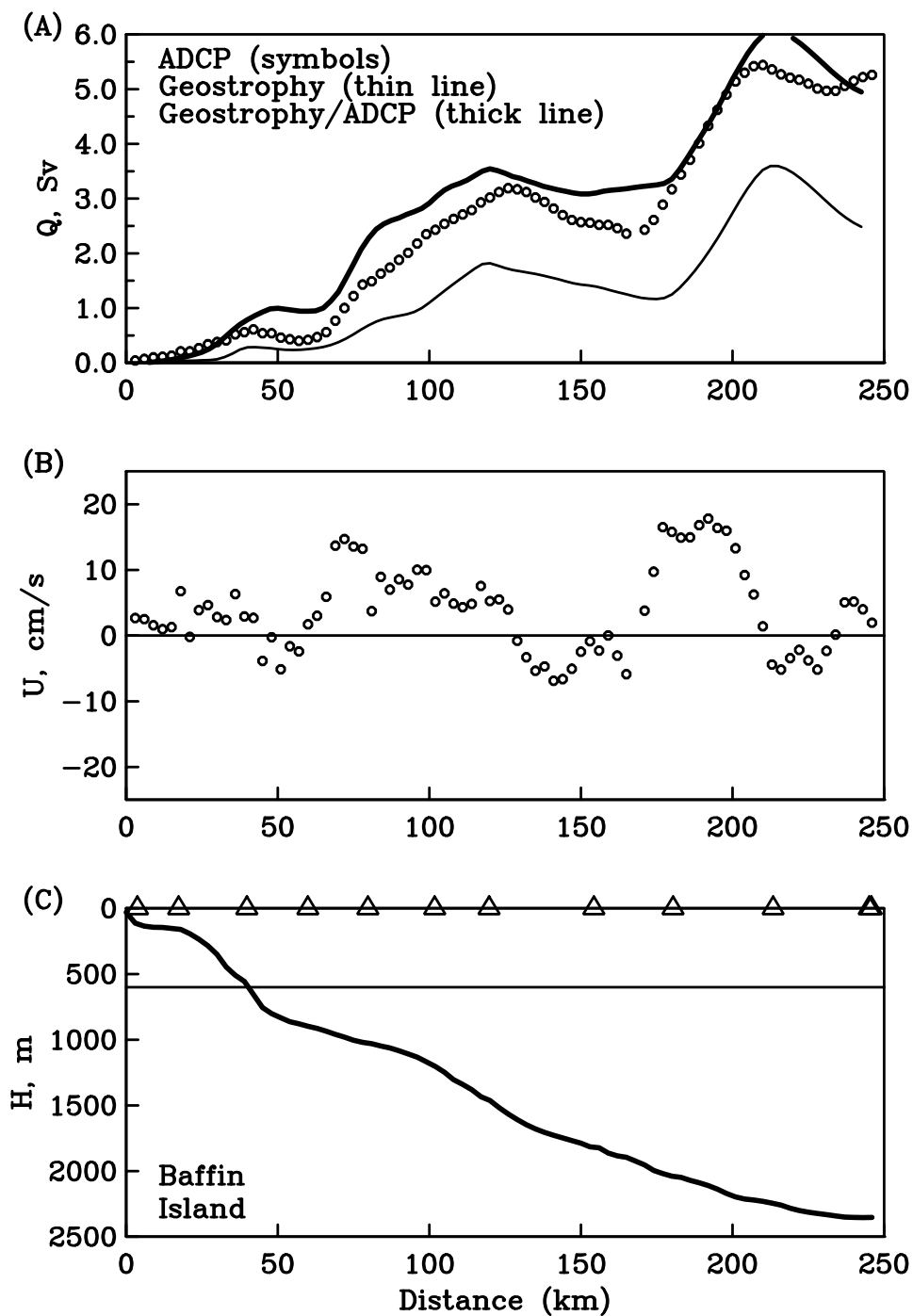


Figure 10: Northern Baffin Island section, July 26/27, 2003: (a) cumulative volume flux over top 600 m from ADCP (symbols) and thermal wind relative to zero flow at bottom or 600-m (thin line) or relative to bottom ADCP (thick line); (b) vertically averaged along-shore ADCP velocity component (symbols), and (c) bottom topography. Symbol indicate CTD station locations, e.g., Fig. 7.

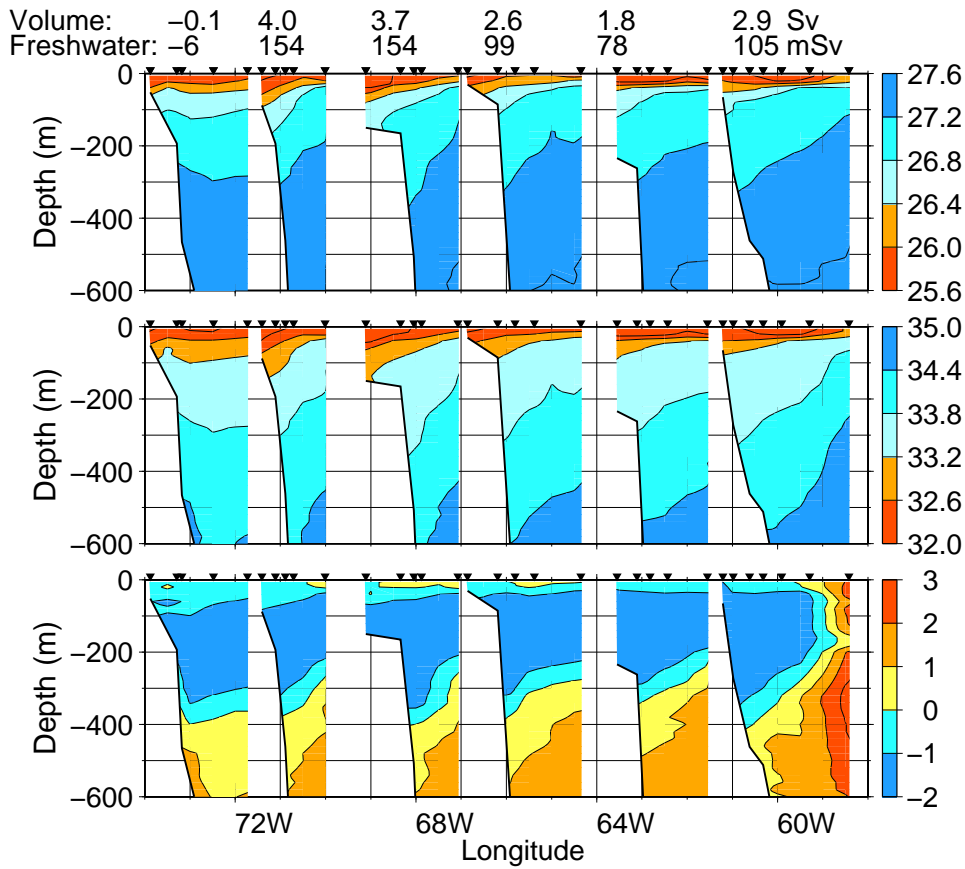


Figure 11: Potential temperature (bottom), salinity (middle), and potential density anomaly (top) along coastal Baffin Island with sections from 72.1°N (left) to 67.1°N (right). The geostrophic volume and freshwater flux estimates are relative to no flow at 600 m depth are shown also. Sections are shown against longitude with 1° representing 38 km at 70°N. Station locations are indicated by small symbols while numbers at the top are geostrophic volume and freshwater flux estimates relative to no flow at 600 m.

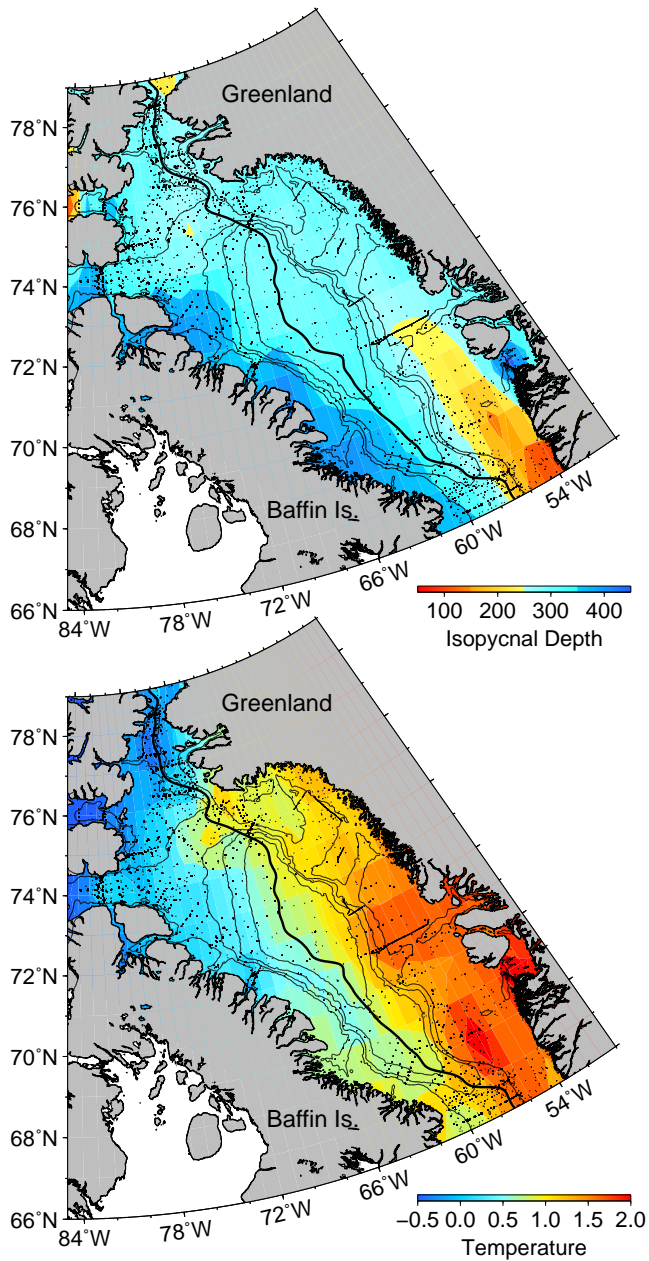


Figure 12: Depth in meters (top) and potential temperature in °C (bottom) on the 1027.4 kg m⁻³ isopycnal shown in color from climatological data over contours of bottom depth from 500 m to 2000 m in 500 m increments. Thick line is the thalweg. Symbols indicate station locations; note the absence of data from the Baffin Island shelf between 69°N and 72°N latitude.

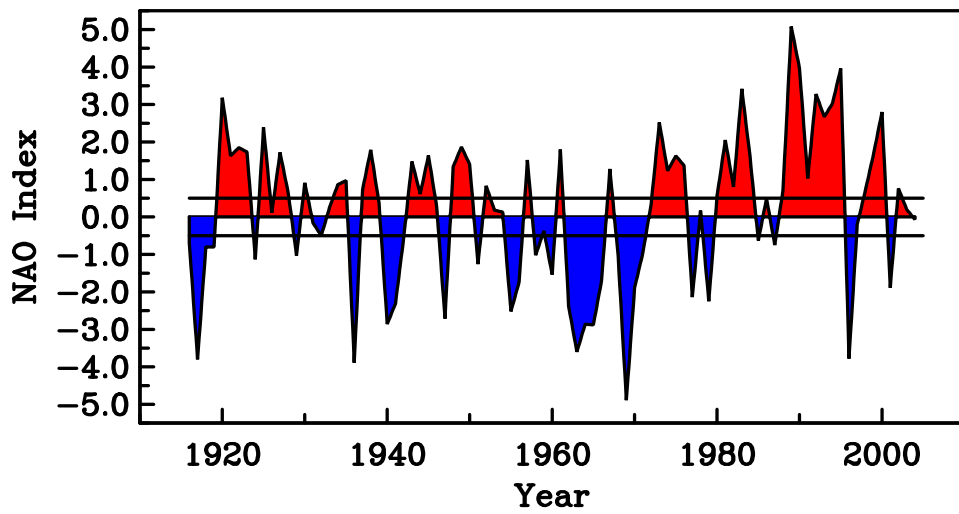


Figure 13: Time series of the North-Atlantic Oscillation index from 1910 through 2004. Horizontal lines at ± 0.5 separate larger positive and larger negative NAO years that we use in the NAO conditional averaging in Fig. 14.

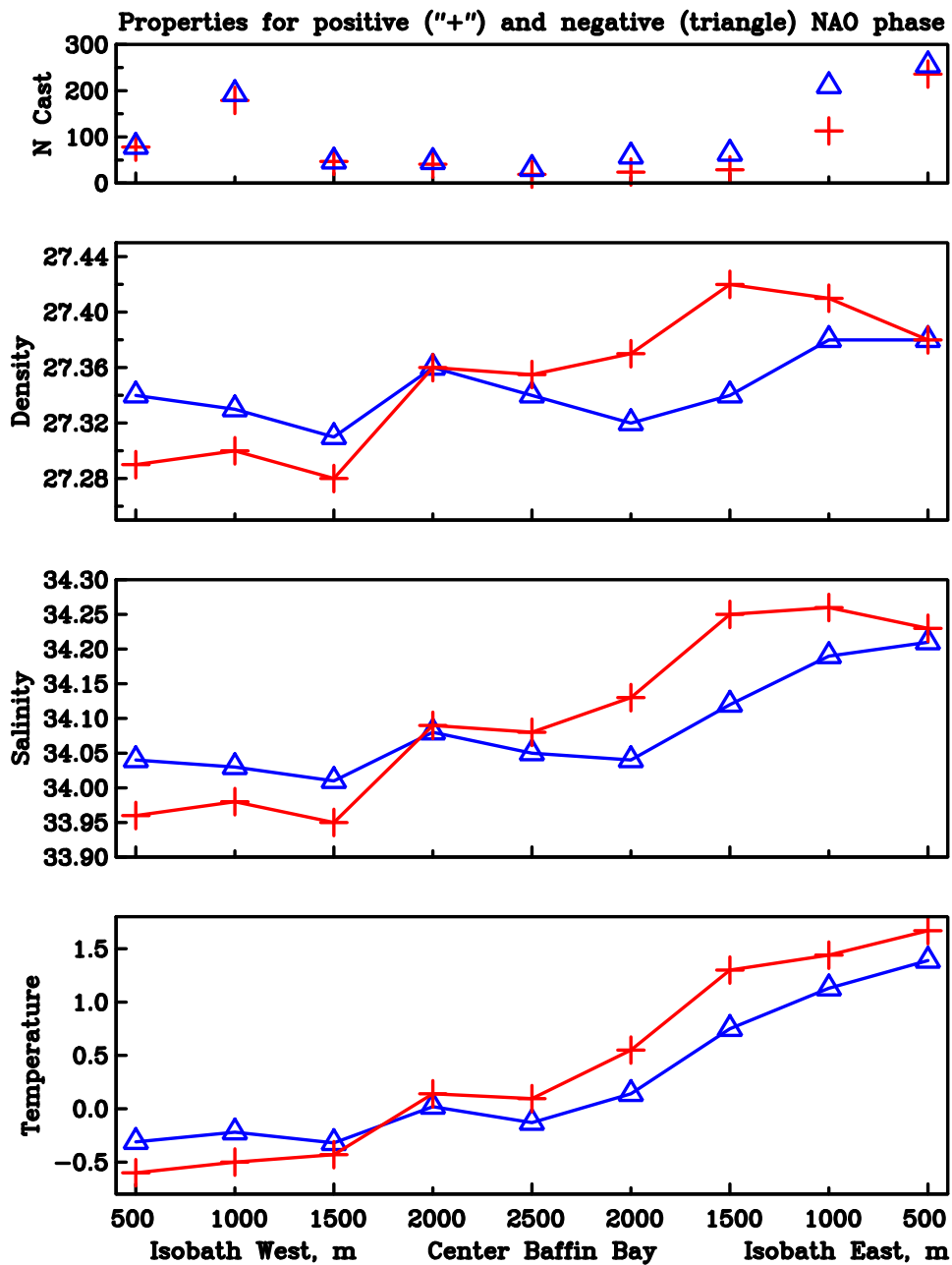


Figure 14: Water properties 200-400 m level across Baffin Bay averaged conditionally for positive and negative NAO phase by bottom depths west (off Canada) and east (off Greenland) of the thalweg. A positive NAO is associated with fresher and cooler waters off Canada and saltier and warmer waters off Greenland relative to a negative NAO. Top panel shows the number of vertical casts entering the average.

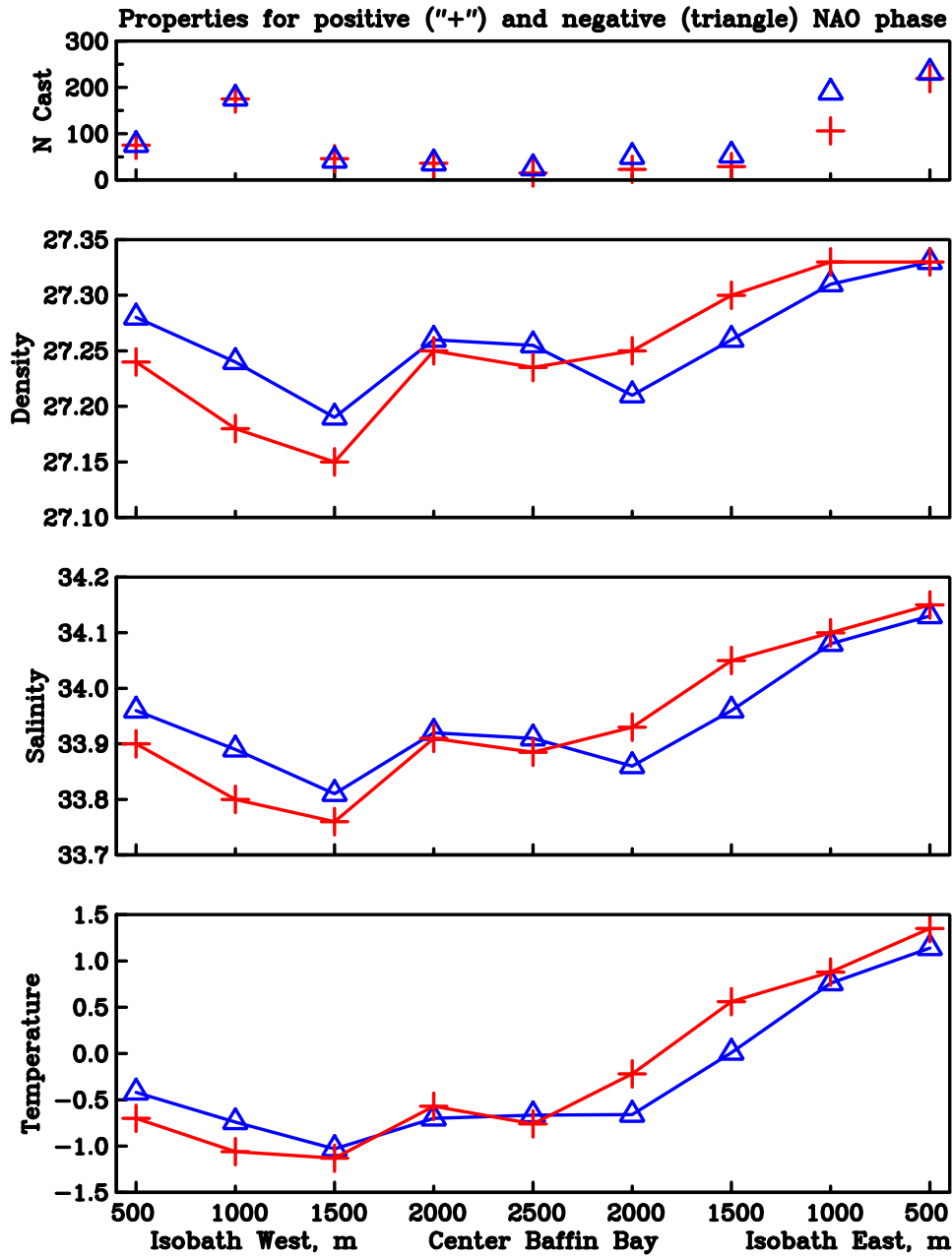


Figure 15: As Figure 14, but for water properties 150-250 m level.